UNIVERSITY OF CALIFORNIA, SAN DIEGO

RPM-1 Suppressors Act in Synapse Formation and Axon Termination in
Caenorhabditis elegans

A dissertation submitted in partial satisfaction of the requirements
for the degree
Doctor of Philosophy

in

Biology

by

Gloriana Victoria Trujillo

Committee in Charge:

　　　Professor Yishi Jin, Chair
　　　Professor Arshad Desai
　　　Professor Gentry Patrick
　　　Professor Nicholas Spitzer
　　　Professor Susan Taylor

2010

UMI Number: 3404415

UMI

Dissertation Publishing

ProQuest®

The Dissertation of Gloriana Victoria Trujillo is approved, and it is acceptable

in quality and form for publication on microfilm and electronically:

_____

_____

_____

_____

<div align="right">Chair</div>

University of California, San Diego

2010

DEDICATION

For all the support and help of family and friends, especially during times when I was losing my motivation, I dedicate this work to you. The Gallegos, Rivera, Trujillo, and Valdez families have been instrumental in my progress and success in graduate school. For all the prayers, novenas, karma and candles burned, I am grateful. This accomplishment would not have been possible without these offerings. To David, thank you for giving me reasons to get it done.

EPIGRAPH

I'm reaching up and reaching out. I'm reaching for the random or what ever will bewilder me.

Maynard James Keenan

TABLE OF CONTENTS

LIST OF FIGURES

LIST OF TABLES

ACKNOWLEDGEMENTS

I would like to acknowledge my advisor, Dr. Yishi Jin, for all the guidance and advice throughout my time in her lab and the transition between institutions midway through my graduate career. Dr. Andrew Chisholm has also been instrumental in introducing important perspectives and generating thoughtful discussion in lab meetings.

The Jin and Chisholm lab members who I overlapped with must be acknowledged for all the helpful suggestions and feedback of my work throughout my time in the lab. They were also crucial in teaching and supporting me, while providing a wonderful lab environment in which to work.

My dissertation committee at UCSD has been invaluable for their support and suggestions over the past three years as a UCSD student.

Chapter 1, in full, has been submitted for publication of the material as it may appear in *Genetics*. The dissertation author was the primary investigator and author of this paper. The work could not have been done without the initiating work and contributions of Dr. Katsunori Nakata with the support of Dr. Ich N. Maruyama. Dong Yan also contributed significant experiments and critical discussion to this manuscript.

VITA

Education

2010 — PhD. Division of Biological Sciences, Neurobiology Section, University

of California, San Diego; La Jolla, CA.

2001 — B.A. Biology, Dartmouth College; Hanover, NH.

Research Experience

2007-present — Graduate Student Researcher - University of California, San

Diego; La Jolla, CA

Dissertation research with Dr. Yishi Jin, designed and

performed experiments investigating synaptogenesis

molecules using genetics and cell biology in *C. elegans*

2003 - 2006 — Graduate Student Researcher - University of California, Santa

Cruz; Santa Cruz, CA

Predoctoral research with Dr. Yishi Jin, designed and

performed experiments investigating synaptogenesis

molecules using genetic screens in

C. elegans

2001 - 2003 — Post-Graduate Researcher - University of California, Davis;

Davis, CA

Research guided by Dr. Noelle L'Etoile, performed

experiments studying olfactory adaptation in *C. elegans*

1999 - 2001 — Undergraduate Student - Los Alamos National Laboratory; Los

Alamos, NM

Research guided by Dr. Fadi Abdi in the lab of Dr. Xian Chen,

performed experiments identifying single nucleotide

polymorphisms using mass spectrometry

Awards and Fellowships

2009-2010 — NSF GK-12 Fellowship, University of California, San Diego

2008 — SACNAS National Conference Travel and Accommodations

Award

2006 — AGEP/NSF Travel Award to attend C. elegans Topic Meeting

2006 — SACNAS National Conference Travel and Accommodations

Award

2003-2005 — Eugene Cota-Robles Fellowship, University of California, Santa

Cruz

Teaching/Mentorship

2009-2010 — Curriculum development and implementation in AP Biology and

Biology classes with Jessica McSwain, MEd at Hilltop High

School through NSF GK-12 Fellowship

2008 — Teaching Assistant, BIMM110: Molecular Mechanisms of

Human Disease with Dr. Immo Scheffler, University of

California, San Diego

2006 — Mentored undergraduate Elizabeth Stepanov, University of

California, Santa Cruz

Publications

Trujillo G.*, Nakata K.*, Yan D., Maruyama I., Jin Y. (submitted to *Genetics*). A
novel ubiquitin E2 variant protein acts in axon termination and synaptogenesis
in C. elegans. GG designed and performed research, analyzed data and wrote
the manuscript.

L'Etoile N.D., Coburn C.M., Eastham J., Kistler A., Gallegos G., Bargmann C.I.
(2001). The cyclic GMP-dependent protein kinase EGL-4 regulates olfactory
adaptation in *C. elegans*. *Neuron* 36, 1079-1089. GG performed research and
analyzed data.

Scientific Community Involvement

2007-present — Volunteer, Salk Mobile Science Lab, various local area middle schools, assisted in hands-on science experiments such as DNA extraction and food coloring electrophoresis

2007, 2010 — Volunteer, San Diego Expanding Your Horizons Day, introduced girls grades 7-12 to science careers

2007-2008 — Volunteer, Salk High School Science Day, introducing local students to Salk Institute

2006 — Judge, Math Science Engineering Achievement (MESA) local and regional competitions

2005-2006 — Participation in Minority Access to Research Careers (MARC) and Minority Biomedical Research Society (MBRS), provided support and guidance for undergraduates

Presentations

Gallegos, G., Nakata, K., Yan, D., Maruyama, Y. and Yishi Jin. Understanding the Role of a Novel Ubiquitin E2 Variant Protein in Axon Termination and Synaptogenesis. St. Jude Children's Research Hospital National Graduate Student Symposium 2009.

Gallegos, G., Nakata, K., Yan, D., Maruyama, Y. and Yishi Jin. Understanding the Role of a Novel Ubiquitin E2 Variant Protein in Axon Termination and Synaptogenesis. Society for the Advancement of Chicanos and Native Americans in Science National Conference 2008.

Gallegos, G., Nakata, K., Yan, D., Maruyama, Y. and Yishi Jin. Understanding the Role of a Novel Ubiquitin E2 Variant Protein in Axon Termination and Synaptogenesis. *C. elegans* Neuronal Development, Synaptic Function & Behavior Topic Meeting 2008.

Gallegos, G. and Yishi Jin. Dissecting the Role of Ubiquitin-Mediated Degradation in Synapse Formation. Society for the Advancement of Chicanos and Native Americans in Science National Conference 2006.

Poster Presentations

Gallegos Trujillo, G., Nakata, K., Yan, D., Maruyama, Y. and Yishi Jin. *C. elegans*: An elegant way to study developmental neurobiology and connect with high school students. National Science Foundation Graduate STEM Fellows in K-12 Education Research Poster Presentation 2010.

Gallegos, G., Nakata, K., Yan, D., Maruyama, Y. and Yishi Jin. Understanding the Role of a Novel Ubiquitin E2 Variant Protein in Axon Termination and Synaptogenesis. St. Jude Children's Research Hospital National Graduate Student Symposium 2009.

Gallegos, G., Nakata, K., Yan, D., Maruyama, Y. and Yishi Jin. A Novel Ubiquitin E2 Variant Protein Acts in Axon Termination and Synaptogenesis in *C. elegans*. Cold Spring Harbor Laboratory 2008 Meeting on Axon Guidance, Synaptogenesis and Neural Plasticity.

Gallegos, G. and Yishi Jin. Identifying Additional Components of the RPM-1 Pathway in Synapse Formation. *C. elegans* Neuronal Development, Synaptic Function, and Behavior Meeting 2006, Abstract 142.

Gallegos, G. and Yishi Jin. Identifying Additional Components of the RPM-1 Pathway in Synapse Formation. 16th International *C. elegans* Meeting 2005.

Nakata, K., Abrams, B., Grill, B., Gallegos, G., Goncharov, A., Huang, X. and Jin, Y. Regulation of a novel MAP kinase cascade by RPM-1 is required for synapse development. West Coast Worm Meeting 2004, Abstract 155.

Gallegos, G.V., and L'Etoile, N.D. egl-4 Mutants Differ in Modulating Olfactory

Adaptation. International Worm Meeting 2003, Abstract 401.

Gallegos, G.V., and L'Etoile, N.D. Modulation of Olfactory Adaptation in C.

elegans. West Coast Worm Meeting 2002, Abstract 113.

Professional Society Membership

2009-present — American Society for Cell Biology

2007-present — Association for Women In Science

2007-present — American Association for the Advancement of Science

2006-present — Society for the Advancement of Chicanos and Native

Americans in Science

2006-present — Alliance for Graduate Education and the Professoriate

(AGEP/NSF)

2003-2004 — Genetics Society of America

ABSTRACT OF THE DISSERTATION

RPM-1 Suppressors Act in Synapse Formation and Axon Termination in
Caenorhabditis elegans

by

Gloriana Victoria Trujillo

Doctor of Philosophy in Biology

University of California, San Diego, 2010

Professor Yishi Jin, Chair

One prevailing question in developmental neurobiology is how neurons form precise connections with their targets. The PHR (Pam/Highwire/RPM-1) protein family is highly conserved from mammals to zebrafish and is important for both axon termination and synapse formation. *Caenorhabditis elegans* RPM-1 (Regulator of Presynaptic Morphology) is a large protein with multiple domains. One role of RPM-1 is to negatively regulate a mitogen-activated protein kinase (MAPK) cascade via proteasomal degradation. To learn more

about the RPM-1 signaling pathway, a genetic suppressor screen was utilized to identify additional molecules downstream of RPM-1. Suppressors were initially tested by non-complementation against known *rpm-1* suppressors to identify novel suppressors.

One such suppressor was further studied and the molecular lesion was identified by single nucleotide polymorphism (SNP) mapping and rescue experiments. *uev-3* is a ubiquitin conjugating E2 variant (UEV) located on Chromosome I. UEV proteins are similar to E2 proteins in the proteasomal degradation pathway, but lack an active cysteine required for its conjugating function. *uev-3* can suppress *rpm-1* defects in both synapse formation in GABAergic motor neurons and axon termination phenotypes in mechanosensory neurons. Using genetic epistasis analysis, *uev-3* was placed in the MAPK pathway downstream of RPM-1 and more precisely, downstream of the MAPKK *mkk-4*. In experiments analyzing relief of suppression of *rpm-1* defects in neurons or muscle, *uev-3* was found to act in presynaptic neurons. Yeast two-hybrid experiments showed that UEV-3 interacts specifically with p38 MAPK PMK-3, and not with any of the other known MAPK pathway members. We hypothesize that the interaction between PMK-3 and UEV-3 results in activation of other, yet unidentified, targets to transduce signals controlling axon termination and synaptogenesis.

Additional novel suppressors of *rpm-1* have been identified via non-complementation tests against known *rpm-1* suppressors. The genes that contain the suppressor lesions have not yet been identified; however, mapping data has narrowed the region containing the suppressors to specific regions of individual chromosomes.

My dissertation provides characterization of a novel protein involved in synaptogenesis and the addition of mapping information for additional proteins important in synapse formation downstream of RPM-1.

INTRODUCTION

A BRIEF OVERVIEW OF SYNAPSE FORMATION

The nervous system has an incredible responsibility to receive, integrate and respond to the mass of information encountered throughout the life of an organism. The nervous system is made up of billions of neurons that interconnect into a network of circuits. Appropriate function of the nervous system is achieved by the formation of structures called synapses. Synapses are the functional units that connect circuits and form between neurons and their targets, which can be another neuron, a muscle or a gland.

Neurons communicate with their target via electrical or chemical synapses. Chemical synapses are asymmetric junctions separated by a synaptic cleft. The presynaptic terminal contains synaptic vesicles filled with neurotransmitter and a region specialized for the docking and fusion of these synaptic vesicles known as the "active zone" (Zhai and Bellen, 2004). The postsynaptic terminal contains the receptors necessary for binding neurotransmitter molecules and relaying the message onto the next cell or target. In order for the process of neurotransmission to function correctly, synaptic proteins must be precisely organized during development.

The process of synapse formation has been described as a five-step process (Garner et al., 2006) beginning when the presynaptic neuron, guided by both attractant and repellant extracellular molecules, finds its correct target.

During the target recognition process, many cell adhesion molecules are important for both recognition and stabilization of the interaction (Giagtzoglou et al., 2009). Once the target has been identified and the interaction between the two has been stabilized, differentiation of both presynaptic and postsynaptic sites occurs. A host of proteins must be shuttled from the cell body to the synapse to construct a functional structure (Jin and Garner, 2008). Upon delivery of the synaptic proteins to the correct compartment, organization of these proteins occurs and culminates in structural and functional maturation (Garner et al., 2006). Finally, the synapse must be maintained for the duration of the life of the synapse through mechanisms that are still under investigation. The theme of my dissertation is to understand the process by which synaptic proteins are organized at the presynaptic terminal.

UTILITY OF GENETIC SCREENS AND *C. ELEGANS*

The soil nematode, *Caenorhabditis elegans*, was initially chosen as an organism to study the function of the nervous system (Horvitz and Sulston, 1990). Serial electron micrograph reconstruction of the nervous system revealed two important findings: that the nervous system of *C. elegans* is relatively simple at 302 total neurons in hermaphrodites, and that the positions of these neurons are invariant (White, 1976). The majority of these neurons are concentrated in a structure known as the "nerve ring" in the anterior region near the head. Affectionately known as "the worm", genetic studies were

conducted to identify genes important for nervous system function by large-scale mutagenesis (Brenner, 1974). *C. elegans* has a rapid generation time and is hermaphroditic, which makes genetic screens scalable to screening thousands of animals and potential mutations (Jorgensen and Mango, 2002). Genetic screens and study of the nervous system were important early in the development of *C. elegans* as a model genetic organism, which are the primary approaches used in my dissertation research.

Transparency and small size are just a few of the attributes that make *C. elegans* the ideal organism to study nervous system development. With the development of green fluorescent protein (GFP) as a tool for biological research (Chalfie et al., 1994), visualization of synaptic components became possible as with a synaptobrevin-GFP marker (Nonet, 1999). Synaptobrevin is an integral membrane protein in synaptic vesicles. The synaptobrevin marker displays accumulations of synaptic vesicles at the presynaptic terminals. Expression of this marker under different neuronal promoters created a tool for mutant hunting via forward genetic screens in specific neuron types (Jin, 2005).

juIs1 is a synaptobrevin-GFP expressed in GABAergic motor neurons. The *juIs1* puncta are present along the dorsal and ventral nerve cords in the worm. *juIs1* has been a useful tool in identifying proteins important for synaptic development through forward genetic screens. Numerous proteins important

for synaptic architectural formation and function have been identified in these mutagenesis screens (Hallam et al., 2002; Zhen et al., 2000; Zhen and Jin, 1999). *syd-2* is a liprin protein identified in one such screen (Zhen and Jin, 1999) important for differentiation of the presynaptic terminal and first identified in yeast two-hybrid studies for interacting with LAR receptor protein tyrosine phosphatases (Serra-Pages et al., 1998).

RPM-1 IS A CONSERVED PROTEIN WITH MULTIPLE ROLES IN NEURONAL DEVELOPMENT

One such protein is *rpm-1*, or Regulator of Presynaptic Morphology, which was initially identified in both *C. elegans* and *Drosophila (highwire)* for its synaptic morphology defects (Schaefer et al., 2000; Wan et al., 2000; Zhen et al., 2000). In *C. elegans*, *rpm-1* mutants have a disorganized pattern of *juIs1*, with some regions containing larger accumulations of the marker, while others contain no evidence of synapses, even at the ultrastructural level (Zhen et al., 2000). Schaefer et al. concurrently identified *rpm-1* using a synaptobrevin-GFP expressed in mechanosensory neurons. Additionally, they showed that *rpm-1* mutants had defective axon termination in mechanosensory neurons when expressing GFP specifically in mechanosensory neurons. *Drosophila highwire* was identified in a screen for synaptic bouton overgrowth (Wan et al., 2000).

RPM-1 is a large protein of 3766 amino acids containing family specific repeats, a guanine-nucleotide exchange factor (GEF) domain, *myc*-binding domain, B-box and a RING-zinc finger domains, characteristic of E3 ubiquitin ligases. Family specific repeats (named PHR for mammalian Pam/Highwire/RPM-1) are important for correct localization of RPM-1. E3 ubiquitin ligases are important for substrate selectivity in the ubiquitin proteasomal degradation pathway (Pickart, 2001). How the function of RPM-1 relates to proteasomal degradation was identified in both *C. elegans* and *Drosophila* experiments. First, a screen looking for synaptic overgrowth in *Drosophila* identified a de-ubiquitinating enzyme, *fat facets*, that also happened to genetically interact with *rpm-1* homolog, *highwire* (DiAntonio et al., 2001). Next, a suppressor screen in *C. elegans* identified an entire mitogen-activated protein kinase (MAPK) cascade as being downstream of *rpm-1* (Nakata et al., 2005). The MAPK cascade is comprised of MAPK kinase kinase (MAPKKK) *dlk-1*, MAPKK *mkk-4*, and MAPK *pmk-3*. In *Drosophila*, the homolog for the MAPKKK, *Wallenda*, was identified soon after, also in a suppressor screen (Collins et al., 2006). However, unlike the findings in worms, the *Drosophila* pathway contains a terminal c-*J*un *N*-terminal *K*inase (JNK) rather than a p38 MAPK. Biochemical evidence has also supported a role for RPM-1 in the proteasomal degradation pathway as partners FSN-

1/*Dfsn/Fbxo45* (Liao et al., 2004; Saiga et al., 2009; Wu et al., 2007) and Skp/Cullin (Liao et al., 2004).

RPM-1 and Highwire belong to the PHR family of proteins for Pam, Highwire and RPM-1 (Po et al., 2010). Conserved proteins include human Pam, murine Phr1, zebrafish Esrom, *Drosophila* Highwire, and *C. elegans* RPM-1. Through biochemical studies, additional signaling pathways and interacting proteins have been identified. These include *myc* (Guo et al., 1998), adenylate cyclase (Scholich et al., 2001), tuberis sclerosis complex (TSC) (Murthy et al., 2004), ALK (Liao et al., 2004), Smad (McCabe et al., 2004), neuronal K^+Cl^- transporter KCC2 (Garbarini and Delpire, 2008), F-actin (Pierre et al., 2008), mTOR (Maeurer et al., 2009) and Rab GEF GLO-4 (Grill et al., 2007). How these pathways may affect synaptogenesis is not yet well understood.

Other neurodevelopmental roles for PHR proteins have come from vertebrate studies in zebrafish and mice. In a mutagenesis screen for motor neuron pathfinding defects, mutants in murine Phr1 incorrectly guide axons to their targets due to defective microtubules in growth cones (Lewcock et al., 2007). Similar defects were observed in cortical axons of a conditional knockout of Phr1 (Bloom et al., 2007). Zebrafish *esrom* was first identified in a screen for aberrant topographic mapping, where the anterior retinal axons fail to map to the posterior tectum (D'Souza et al., 2005).

To learn more about the effects of RPM-1 on synapse formation and axon termination, *rpm-1* suppressors have again proven useful. Recently, two novel suppressors of *rpm-1* were identified as part of the DLK-1 MAPK pathway and found to act downstream of PMK-3 (Yan et al., 2009). *mak-2* is a MAPK-activated protein kinase and *cebp-1* is a CCAAT/enhancer binding protein transcription factor, which contains a basic-leucine-zipper domain. *mak-2* and *cebp-1* are both present in the presynaptic terminal. The DLK-1 pathway was shown to be necessary for regeneration of severed neurons (hammarlund ref), so to are *mak-2* and *cebp-1* important in this process (Yan et al., 2009). The upstream DLK-1 MAPK cascade was found to regulate *cebp-1* mRNA via its 3'UTR (Yan et al., 2009). Interesting next steps include identifying the transcriptional targets of CEBP-1. Thus, unmasking the role of RPM-1 in synapse formation and axon termination has been further characterized by the identification of *rpm-1* suppressors.

In the following chapters, I describe the identification of an additional *rpm-1* suppressor, *uev-3,* and the mapping and characterization of additional suppressors. Finally, I describe a small-scale RNAi screen that was initiated to identify more members of the RPM-1 pathway via a candidate gene approach.

CHAPTER 1: A NOVEL UBIQUITIN E2 VARIANT PROTEIN ACTS IN AXON TERMINATION AND SYNAPTOGENESIS IN *C. ELEGANS*

ABSTRACT

In the developing nervous system, cohorts of events regulate the precise patterning of axons and formation of synapses between presynaptic neurons and their targets. The conserved PHR proteins play important roles in many aspects of axon and synapse development from *C. elegans* to mammals. One of the functions for PHR proteins is to act as E3 ubiquitin ligases for the dual-leucine-zipper-bearing MAP kinase kinase kinase (DLK MAPKKK) to regulate a MAP kinase signal transduction cascade. In *C. elegans,* loss of function of the PHR protein RPM-1 (Regulator of Presynaptic Morphology-1) results in formation of fewer synapses, disorganized presynaptic terminal architecture, and frequent axon overextension. Inactivation of the DLK-1 pathway suppresses these defects. By characterizing additional genetic suppressors of *rpm-1*, we present here a new member of this DLK-1 pathway, *uev-3*, an E2 ubiquitin conjugating enzyme variant. We show that *uev-3* acts cell autonomously in neurons, despite its ubiquitous expression. Our genetic epistasis analysis supports a conclusion that *uev-3* acts downstream of the MAPKK *mkk-4*, and upstream of the MAPKAPK *mak-2*. UEV-3 can interact with the p38 MAPK PMK-3 in a yeast

two-hybrid assay. Studies using chimera UEV transgenes support that the UEV domain is necessary for the function of UEV-3. We postulate that UEV-3 may provide additional specificity in the DLK-1 pathway by contributing to activation of PMK-3 or limiting the substrates accessible to PMK-3.

INTRODUCTION

Neurons communicate with their targets via specialized junctions known as synapses. Synapses send chemical messages between synaptic contacts or electrical messages through gap junctions. At chemical synapses an electrical impulse causes calcium channel opening and consequently stimulates synaptic vesicles residing in the presynaptic terminals to fuse at the plasma membrane. Neurotransmitter activates receptors on the postsynaptic membrane and triggers signal transduction in the target cell. In order for this communication to occur both correctly and efficiently, the organization of the proteins within these juxtaposed terminals must be tightly regulated (Jin and Garner, 2008). Genetic approaches in *C. elegans* have identified molecules in the presynaptic terminal important for this organization, such as RPM-1, a member of the PHR family of proteins (Schaefer et al., 2000; Zhen et al., 2000).

The PHR (for Pam/Highwire/RPM-1) protein family includes human Pam, murine Phr1, Zebrafish Esrom/Phr, *Drosophila* Highwire and *C. elegans*

RPM-1. PHR family members are important for axon guidance, axon growth and synapse formation (Bloom et al., 2007; D'Souza et al., 2005; Grill et al., 2007; Lewcock et al., 2007; Li et al., 2008; Nakata et al., 2005; Po et al.). The signaling cascades regulated by the PHR proteins have recently been identified using genetic modifier screens (Collins et al., 2006; DiAntonio et al., 2001; Liao et al., 2004; Nakata et al., 2005) and biochemical approaches (Grill et al., 2007; Wu et al., 2007). In *C. elegans*, RPM-1 negatively regulates a p38 mitogen-activated protein kinase (MAPK) cascade that contains MAPK PMK-3, MAPKK MKK-4, and MAPKKK DLK-1. RPM-1 negatively regulates this cascade by ubiquitinating DLK-1, which results in proteasomal degradation of DLK-1 (Nakata et al., 2005). The DLK-1 cascade further activates a MAPK-activated protein kinase (MAPKAPK) MAK-2, to regulate the activity of a transcription factor of the CCAAT/enhancer binding protein (C/EBP) family, CEBP-1 (Yan et al., 2009).

It is widely known that signal transduction cascades involving MAP kinases are fine-tuned using multiple mechanisms to ensure optimal signaling outputs (Raman et al., 2007). For example, scaffold proteins for MAP kinases can provide spatial regulation of kinase activation in response to different stimuli (Remy and Michnick, 2004; Whitmarsh, 2006). Small protein tags such as ubiquitin have also been shown to control the activation of kinases. Specifically, in the IKK pathway ubiquitination via Lys63 chain formation

catalyzed by the Ubc13/Uev1a E2 complex and TRAF6 E3 ligase is required for TAK1 kinase activation (Skaug et al., 2009).

To further the understanding of the RPM-1 and DLK-1 pathway in the development of the nervous system, we characterized a new complementation group of *rpm-1(lf)* suppressors. We show that these mutations affect the gene *uev-3*, a novel ubiquitin E2 conjugating (UBC) enzyme variant (UEV). Similar to other members of the DLK-1 pathway, *uev-3* functions cell autonomously in neurons. *uev-3* genetically acts downstream of *mkk-4* and upstream of *mak-2*. In the yeast two-hybrid assay, UEV-3 interacts with PMK-3. UEV proteins belong to the UBC family, but lack the catalytic active cysteine necessary for conjugating ubiquitin (Sancho et al., 1998). Using domain swapping experiments, we provide evidence that the UEV domain of UEV-3 likely functions in a manner resembling canonical UEV proteins. We hypothesize that UEV-3 may be acting to add specificity to the DLK-1 pathway by binding to PMK-3 for its activation or for selecting specific downstream targets.

MATERIALS & METHODS

C. elegans genetics: *C. elegans* strains were maintained as described (Brenner, 1974). The suppressors were isolated from *rpm-1(ju44); syd-2(ju37); juIs1* or *rpm-1(ju44); syd-1(ju82); juIs1* animals mutagenized with 50 mM EMS (Nakata et al., 2005). Suppressor mutations were outcrossed

multiple times against wild type (N2) or *juIs1* strains. Specificity of

suppression of *rpm-1(lf)* was tested by crossing *sup; rpm-1; syd-2; juIs1* to

rpm-1; juIs1 males. Double mutant constructions were carried out following

standard procedures, and the genotypes were confirmed by allele-specific

nucleotide alterations determined by DNA sequencing or restriction enzyme

digest.

Cloning of *uev-3*: We mapped the suppression activity of *uev-3(ju587)*

in the *rpm-1; syd-2* double mutant strain to Chromosome I near +4 using the

single-nucleotide polymorphism mapping strategy (Davis et al., 2005; Nakata

et al., 2005). For fine mapping of *uev-3 (ju587)*, we constructed *dpy-5 uev-3*

(ju587) unc-75; rpm-1; juIs1 strain. Following crossing to the Hawaiian strain

CB4856, recombinant animals of phenotypic Dpy non-Unc or Unc non-Dpy

that were mutant for *rpm-1* were selected, and the presence of *uev-3 (ju587)*

in each recombinant was determined by observing *juIs1* marker expression.

uev-3 (ju587) was mapped between *snp_F14B4[1]* and *snp_M04C9[1],* within

a 90 kb interval including about 19 predicted genes. We did RNAi against the

predicted genes using a sensitized strain *eri-1(mg366); rpm-1(ju23); syd-*

2(ju37), and found that *uev-3* RNAi partially suppressed *rpm-1; syd-2*

phenotypes*. ju593, ju638,* and *ju639* were determined to be alleles of *uev-3*

based on linkage to chromosome I and non-complementation test. DNA

sequence analyses of these suppressor mutations were carried out following

standard procedures, and the nucleotide alterations were confirmed in
independent PCR reactions.

Molecular biology and expression constructs: We determined the gene
structure and the full-length transcripts of *uev-3* by performing RT-PCR and 5'
RACE analyses. Total RNAs were prepared using TRIzol reagents
(Invitrogen, Carlsbad, CA) according to the manufacturer's instructions, and
cDNAs were generated using Superscript II reverse transcriptase (Invitrogen,
Carlsbad, CA). 5' RACE kit (Roche Applied Science, Indianapolis, IN) was
used with the following pair of primers to amplify the 5' region of *uev-3:* SP1
and YJ3861 ccattgacacgttgagattc; and SP2 and YJ3846 acgtttagacactcctccc.
DNA sequence analysis of eight cloned 5' RACE products revealed a SL2
splice leader in all, indicating that *uev-3* is transcribed as the downstream
gene in the operon with *rab-5*. We obtained full-length *uev-3* cDNA by RT-
PCR using YJ3852 ggggacaagtttgtacaaaaaagcaggctccaaaatgtccgatcaacctgg
and YJ3853 ggggaccactttgtacaagaaagctgggttatgaaattccaatgacatc. The DNA
sequences of the cDNA clone (pCZ729) were determined, which verified and
corrected the predicted *uev-3* exon and intron boundaries. The *uev-3*
expression constructs in *C. elegans* were generated following standard
procedures or using Gateway Cloning Technology (Invitrogen, Carlsbad, CA),
and the details of the clones are in Table 2. For yeast two-hybrid studies, full
length cDNA or fragments of cDNA for *dlk-1, mkk-4, pmk-3, mak-2,* or *uev-3*

were cloned to either pBTM116 vector to be expressed as GAL4 activation

domain fusion protein, or into pACT2 vector to be expressed as LexA DNA

binding domain fusion protein, as described in Table 2.

Neuronal morphology and synapse analyses: We observed GFP or

SNB-1::GFP using *muIs32[Pmec-7-GFP] or juIs1[Punc-25-SNB-1::GFP]* in

one-day old adult animals either live or anesthetized in 1% 1-phenoxy-2-

propanol (TCI America, Portland, OR) in M9 buffer. Images were captured

either on a Zeiss Axioplan 2 microscope with Chroma HQ filters or a Zeiss

LSM510 confocal miscroscope.

Germline transformation and transgenic analyses: Transgenic animals

were usually generated by injecting DNA at a dilution series (1 ng–50 ng/*μ*l)

following standard procedures (Mello et al., 1991), using either pRF4 *rol-6(dm)*

or *Pttx-3-RFP* as coinjection markers. For each construct, two to thirteen

independent transgenic lines were analyzed.

Yeast two hybrid: Yeast two-hybrid assays were performed using

pACT2 and pBTM116 vector backbones (Clontech, Mountain View, CA). The

yeast strain L40 [*MATa his3D200 trp1-901 leu2-3, 112 ade2 LYS2::(lex-*

Aop)4-HIS3 URA3::(lexAop)8-lacZ GAL4 gal80] was used. The yeast

transformation was performed by the lithium acetate method and selected on

Trp-, Leu-, and His-selection plates. Pairs of plasmids were co-transformed

into yeast strain L40, and selected on –Leu –Trp plates. For interaction assay,

single clones were picked from each transformation and cultured to OD_{600} = 1.

Yeast cells were pelleted by centrifugation, washed 3 times and resuspended,

and plated in a dilution series of 10 to 10000 times by pipeting 5 μl per spot

onto Histidine selection plates containing 3mM 3-AT. ß-galactosidase assays

were performed following the Clontech Yeast Protocols Handbook (Fields and

Sternglanz, 1994).

cebp-1 mRNA analysis by qRT-PCR: Total RNA was isolated using

TRIzol (Invitrogen, Carlsbad, CA) from mixed stage worms cultured under

identical conditions. 5 µg of total RNA was reverse transcribed into cDNA

using an oligo dT primer (Invitrogen, Carlsbad, CA). Power SYBR® Green

PCR Master Mix kits (Applied Biosystems, Foster City, CA) were used for the

PCR reactions and the ABI Prism® 7000 Sequence Detection System was

used for real time PCR. cDNAs were amplified using following primers: *cebp-1*

pair (gcacgacaagatgaagagg and gcatgcgttgctctttca) amplifies 183 bp; *ama-1*

pair (actcagatgacactcaacac and gaatacagtcaacgacggag) amplifies 128 bp.

Statistical analysis: For comparisons of two groups (puncta counts or

RNA transcript ratios) we used a two-tailed Student's t test in Graphpad Prism

(GraphPad Software, La Jolla, CA). For comparison of axon termination

proportions, we used the Fischer Exact Test in GraphPad InStat (GraphPad

Software, La Jolla, CA).

RESULTS

UEV-3 is a novel Ubc/E2 variant protein: A large number of genetic suppressors of *rpm-1* loss of function (lf) mutants were isolated using a sensitized genetic background (Nakata et al., 2005). Among the remaining unknown suppressor mutations, we identified four alleles that belong to the same complementation group: *ju593, ju587, ju638,* and *ju639*. We mapped the suppressor locus to the right arm of Chromosome I between *snp_F14B4[1]* and *snp_M04C9[1]* (Figure 1A). We used a combination of RNAi and transgenic expression of cosmid DNAs from the region of interest to locate the gene affected. We found that a 6kb *Eco*105I - *Spe* I fragment of the cosmid F26H9 contained the rescuing activity for the suppression of *rpm-1(ju44)* by *ju587*. The genomic DNA fragment contains two predicted genes: *rab-5* and *uev-3*. We performed RT-PCR and 5' RACE analyses, and determined that *uev-3* transcripts contained an SL2 splice leader, confirming that *rab-5* and *uev-3* form an operon, with *uev-3* as the downstream gene (Materials & Methods). DNA sequence analysis from *ju587, ju593,* and *ju638* identified single nucleotide alteration at various splice acceptor sites, while *ju639* is a 26 base pair deletion in the sixth exon (Figure 1B, Table 1). The molecular lesions are consistent with these mutations causing loss of function in *uev-3*.

uev-3 is one of the three ubiquitin-conjugating (UBC) E2 enzyme variant (UEV) proteins in *C. elegans* (Jones et al., 2002; Kipreos, 2005). It is

composed of 356 amino acids, with the UEV domain from residues 168 to 324

(Figure 1B). UEV proteins are similar to UBC E2 enzymes but lack the critical

cysteine residue that is required for a transient interaction between E2 and

ubiquitin (Pickart and Eddins, 2004; Sancho et al., 1998). Alignment of the

UEV domain of UEV-3 with other UBC and UEV proteins reveals motifs with

high similarity; for example, the HxN tripeptide motif, which is important for

proper folding of the active site region in UBC proteins, is conserved in UEV-3

(Figure S1) (Gudgen et al., 2004). The overall sequence of UEV-3 is most

similar to *C. elegans* UEV-2, followed by UBC-3 and UBC-7 in *C. elegans*

(Figure 1C).

uev-3(lf) suppresses the phenotypes in motor and mechanosensory

neurons of *rpm-1(lf)*: *rpm-1(lf)* mutants display irregularly shaped and sized

presynaptic terminals in the GABAergic motor neurons (Zhen et al., 2000).

The mutants also show defects in ALM and PLM mechanosensory axon

termination, which is characterized by overextension of ALM and ventral

hooking of PLM, and absence of PLM synaptic branch (Schaefer et al., 2000).

Despite these defects, *rpm-1(lf)* animals appear superficially wild type in the

overall nervous system architecture and locomotory behavior. The *uev-3*

mutants alone also develop normally, and exhibit no discernable abnormalities

in the motor and mechanosensory neurons (Figure 2). However, in an *rpm-*

1(lf) background, mutations in *uev-3* can ameliorate the defects in motor

neuron synapses and touch axon patterning*.*

We determined the extent of *rpm-1(lf)* suppression by *uev-3(lf).* We first

analyzed the presynaptic puncta patterns and numbers using *juIs1 [Punc25-*

SNB-1::GFP], a marker that visualizes presynaptic terminals in GABA motor

neurons (Hallam and Jin, 1998). In wild-type animals, this marker shows a

pattern of uniformly sized and spaced fluorescent puncta along the dorsal and

ventral cords, and on average, 158.9 puncta are visible in the dorsal cord

(Figure 2A). *rpm-1* mutants have fewer puncta, averaging 87.1 puncta in the

dorsal cord. The remaining GFP puncta in *rpm-1* mutants are often enlarged,

and disorganized in distribution. Single mutants of *uev-3(ju587)* or *uev-*

3(ju639) have an average 165.9 or 160.4 puncta per dorsal cord, respectively,

and SNB-1::GFP puncta patterns are similar to wild-type. Both *uev-3(ju587);*

rpm-1(lf) and *uev-3(ju639); rpm-1(lf)* animals show significant suppression of

the *rpm-1* phenotype, increasing SNB-1::GFP puncta number to an average of

116.9 and 111.6 in the dorsal cord, respectively. We also examined the touch

neuron morphology using the *muIs32* [*Pmec-7-GFP]* marker (Ch'ng et al.,

2003). In wild-type animals, the ALM cell body lies laterally in the mid-body

region and sends a longitudinal axonal projection anterior into the pharyngeal

region of the animal where a process branches into the nerve ring and forms

synapses (Figure 2B). The PLM cell body resides in the tail and sends a

projection anterior into the mid-body of the animal, terminating posterior to the ALM cell body. PLM cells also extend a synaptic branch that is directed toward the ventral cord, where it synapses onto its partners. In *rpm-1(lf)* mutants, ALM axons overextend and hook in 61% of animals, the PLM synaptic branch is frequently missing (41.4%), while 79.7% PLM exhibit axon overextension defects in which the axon frequently grows ventrally before terminating, described as "PLM hooking" (Figure 2B). Although low levels of ALM and PLM defects (about 1-4%) are detected in both *uev-3(ju587)* and *uev-3(ju639)* mutants, both mutations significantly suppressed *rpm-1(lf)*. In *uev-3(ju587); rpm-1* mutants only 4.9% do not have the PLM synaptic branch and 19.4% show PLM and ALM hooking. In *uev-3(ju639); rpm-1* the suppression of PLM synaptic branch defects is almost complete, and ALM and PLM hooking is suppressed down to 26.5% and 2.9%, respectively. These data show that the degree of suppression of *rpm-1(lf)* by both alleles of *uev-3* is comparable to those observed for the mutants in the DLK-1 MAPK cascade (Nakata et al., 2005). *uev-3(ju639)* has a slightly stronger suppression effect on the mechanosensory neuron phenotypes, so we have designated *ju639* as the null mutation of the gene.

    <u>*uev-3* acts cell autonomously in presynaptic neurons:</u> We determined the transcriptional expression pattern of the *rab-5* and *uev-3* operon using 1.8 kb of the 5' upstream sequences of the operon to drive GFP expression. GFP

is observed in all tissues, and noticeably present in ventral cord neurons

(Figure 3A). We next addressed whether UEV-3 acts cell autonomously in

neurons by expressing *uev-3* cDNA driven by tissue-specific promoters in *uev-3; rpm-1* mutants (Tables 2, 3). We examined functional rescue of the motor

neuron synaptic phenotypes by quantitating SNB-1::GFP puncta numbers

(Figure 3B). In wild type animals, 22.3 puncta per 100μm are present, while

there are 13.1 puncta in *rpm-1(lf)*. *uev-3(ju587)* have 21.3 puncta per 100μm,

and *uev-3(ju587); rpm-1* suppress *rpm-1(lf)* puncta numbers to 17.8 puncta

per 100μm. Expression of *uev-3* driven by a pan-neuronal promoter, or a

motor neuron specific promoter rescues the suppression of *rpm-1(lf)* to 13.2

and 11.6 puncta per 100μm, respectively, which is comparable to that of

transgenic expressing *uev-3* genomic DNA (13.8 puncta per 100 μm). The

muscle promoter driven transgene did not show any effects on the

suppression in *uev-3; rpm-1* mutants, with 16.4 puncta per 100μm. Similarly,

we expressed *uev-3* cDNA in touch neurons, and observed significant rescue

of the suppression on the mechanosensory neuron phenotypes, as the

transgene-carrying *uev-3; rpm-1* animals showed 55.3% PLM hooking defects

(Figure 3C). As in motor neurons, the muscle-driven promoter did not show

any rescue activity in *uev-3; rpm-1* mutants. The transgenes alone or in a

uev-3 background did not cause any significant defects (Figure 3C, data not

shown for *[Pmyo-3-uev-3]* and *[Prgef-1-uev-3]* transgenes alone). These

results thus demonstrate that *uev-3* is required cell autonomously in presynaptic neurons.

uev-3 acts downstream of mkk-4, upstream of mak-2 in the DLK-1 _MAPK cascade:_ To learn how *uev-3* functions in the DLK-1 MAPK cascade, we performed four lines of experiments. First, we made pair-wise loss of function mutant combinations between *uev-3* and the MAPK genes, and measured the suppression of motor neuron puncta numbers in *rpm-1(lf)* (Figure 4A). For example, *uev-3; rpm-1* have 116.9 SNB-1::GFP puncta per dorsal cord, and *pmk-3; rpm-1* have 130.7 puncta per dorsal cord. The triple mutants *uev-3; pmk-3; rpm-1* show a mean 129.9 puncta number in the dorsal cord, and do not suppress *rpm-1* any stronger than either double mutants. This analysis is consistent with the interpretation that *uev-3* acts in the same pathway with MAPK genes *dlk-1, mkk-4,* and *pmk-3*.

Second, to place *uev-3* within the DLK-1 MAPK pathway, we took advantage of the observations that transgenic expression of either wild type *mkk-4(++)* or a phospho-mimetic *mkk-4(DD)* in a wild type background causes gain of function phenotypes (Nakata et al., 2005). The animals carrying these extra-chromosomal arrays display an uncoordinated movement, with disorganized synaptic puncta resembling those of *rpm-1(lf)* (Figure 4B). Loss of function in *pmk-3*, a gene downstream of *mkk-4,* can suppress both the synaptic and behavior defects associated with either *mkk-4(++)* or *mkk-4(DD)*

transgene, whereas loss of function in *dlk-1,* which acts upstream of *mkk-4,* only suppresses the effects of *mkk-4(++)* (Nakata et al., 2005). We found that when either the *mkk-4(++)* or *mkk-4(DD)* array is in the *uev-3(lf)* background, the body size and movement phenotypes of the transgenes are abolished, and the average total synaptic GFP puncta are increased to 100.5 and 153, respectively. Thus, *uev-3* behaves genetically similar to *pmk-3* and likely acts downstream of *mkk-4.*

Third, we have recently identified that the MAP kinase activated protein kinase MAK-2 and the transcription factor CEBP-1 function downstream of PMK-3 (Yan et al., 2009). To test how *uev-3* interacts with *mak-2* and *cebp-1*, we took advantage of transgenic overexpression of a phospho-mimetic MAK-2, *mak-2(EE)* (Yan et al., 2009)(Figure 4C). For example, in the mechanosensory neurons, animals carrying *mak-2(EE)* transgenes have 77.4% PLM overshooting defects, which are suppressed to 27.8% by loss of function in *cebp-1* but not *pmk-3*. We found that in *uev-3* mutant background *mak-2(EE)* gain of function defects are not suppressed (Figure 4C), consistent with a conclusion that *uev-3* likely acts upstream of *mak-2*.

Lastly, we examined the levels of *cebp-1* mRNA transcripts in *uev-3* backgrounds. One way by which the DLK-1 MAP kinase cascade regulates *cebp-1* is to activate MAK-2, which in turn controls the levels of *cebp-1* mRNA (Yan et al., 2009). We performed quantitative RT-PCR on RNAs isolated from

mixed-stage animals, and compared the levels of *cebp-1* transcripts to those

of the internal control *ama-1,* the large subunit of RNA polymerase II (Sanford

et al., 1983). In *rpm-1* mutants, *cebp-1* transcript levels are elevated

compared to wild type because DLK-1 is not degraded, allowing high-level of

MAP kinase signaling to promote the stability of *cebp-1* mRNA (Figure 4D). In

both *rpm-1; dlk-1* and *rpm-1; uev-3* mutant strains, the transcript levels of

cebp-1 are comparable to wild type levels. All together, these data strongly

support the conclusion that *uev-3* functions in the DLK-1 MAPK pathway, at

the step between *mkk-4* and *mak-2*.

The divergent UEV domain of UEV-3 likely functions in a manner

similar to the conserved UEVs: Biochemical studies of canonical UEV proteins

in yeast and mammalian cells, such as Mms2 and Uev1A, respectively, have

established that the UEV domain functions as an obligatory subunit for an

active Ubc, Ubc13 (Broomfield et al., 1998; Deng et al., 2000; Xiao et al.,

1998). The UEV1A/Ubc13 E2 complex catalyzes Lys63 poly-ubiquitin chain

formation (Hofmann and Pickart, 1999; VanDemark et al., 2001). The ortholog

of Mms2 or Uev1A in *C. elegans* is UEV-1, which can interact with UBC-13

(Gudgen et al., 2004). The UEV domain of the UEV-3 is very divergent from

the canonical UEV (Figure 1C, Figure S1), and also shows limited degree of

similarities to that of UEV-1 (14.7% identity and 30.6% similarity) (Figure 5A).

Residues known to be important for Uev1 binding to either its cognate Ubc13

or ubiquitin do not seem to be conserved in UEV-3 (Moraes et al., 2001; VanDemark et al., 2001) (Figure 5A). In addition, UEV-3 has extended sequences N- and C-terminal to the UEV domain. The sequence comparisons raise the question whether UEV-3 may retain functions similar to those of UEV proteins in other organisms.

We first tested whether *uev-1* interacts with *rpm-1.* The *uev-1* gene resides in an operon as the upstream gene, and its coding sequences are less than 1kb (Figure 5B). We obtained a deletion allele, *ok2610,* which deletes 496bp starting 142 bp in the promoter of the operon and ending 69bp in the third exon of *uev-1* (Figure 5B). The homozygous *ok2610* animals are viable, develop normal touch neurons, and do not suppress *rpm-1(lf)* (Figure 5D). We then tested whether the UEV domain in UEV-3 has a conserved function by generating a chimera gene in which we replaced the UEV domain and C-terminus of UEV-3 with the UEV domain from UEV-1 (Figure 5C). We found that transgenic expression of this UEV chimera protein in neurons shows functional rescue of the suppression of *rpm-1(lf)* in the *uev-3; rpm-1* background to similar levels as does the expression of the full-length *uev-3* (Figure 5D). This result suggests that despite its divergency, the UEV domain of UEV-3 likely has a function similar to that of the canonical UEV domain of UEV-1. However, overexpression of full-length UEV-1 alone in *uev-3; rpm-1* background did not show significant rescue of the suppression of *rpm-1(lf)*

(Figure 5D). Thus, these data suggest that the UEV domain is functionally important for UEV-3, but the regions N- and C-terminal extended sequences may likely convey specificity for the function of UEV-3. To test this, we generated a deletion construct lacking the N-terminal sequences of UEV-3 (aa6-167) (Figure 5C). Transgenic expression of this construct under the control of a pan-neuronal promoter in *uev-3(ju639); rpm-1(lf)* animals exhibit partial rescuing activities, as five out of thirteen independently-derived transgenic lines exhibit PLM hooking phenotypes that are significantly different from *uev-3(ju639); rpm-1(lf)* (representative line shown in Figure 5D). With the caveat of overexpression, this result suggests that the N-terminus of UEV-3 is not absolutely critical, but contributes to its function. It remains possible that combinatorial effects of N- and C-terminus of UEV-3 may provide the optimal specificity of its activity.

UEV proteins are known to act together with an active UBC E2 to ubiquitinate substrates by elongating ubiquitin chains at lysine-63 (Hofmann and Pickart, 1999; Pickart and Eddins, 2004). *C. elegans* has 22 annotated UBC genes. We wanted to test whether UEV-3 might require any UBC. We analyzed available deletion or mutant alleles for several UBC genes including *ubc-13,* and observed no genetic interactions with *rpm-1(lf)* (Table 1). We also performed dsRNAi for 19 *ubc* genes in *eri-1; rpm-1; muIs32* strain and observed that none showed detectable suppression of *rpm-1(lf)* (data not

shown). We also tested protein interactions between UEV-3 and UBC genes using yeast two hybrid assays, and were not able to detect a positive interaction with UEV-3, out of eleven UBC genes and two UEV genes tested (data not shown). In conclusion, our chimeric expression studies support a scenario in which the UEV domain of UEV-3 may have a canonical function like UEV-1. However, UEV-3 might likely have distinct partners for its function.

UEV-3 can bind PMK-3: The UEV protein, Fts1, has been shown to act as a scaffold between protein kinase B (PKB/Akt) and 3-phosphoinositide-dependent kinase 1 (PDK1) (Remy and Michnick, 2004). To better characterize the relationship between UEV-3 and the DLK-1 MAPK cascade, we asked whether UEV-3 could interact with the kinases by performing yeast two-hybrid assays between UEV-3 and all four kinases and CEBP-1. We detected interactions between UEV-3 and PMK-3, but not between UEV-3 and the other three kinases or CEBP-1 (Figure 6A, data not shown for *dlk-1, mkk-4, cebp-1*). We attempted to narrow down the interacting domains using bait expressing only the UEV domain or N-terminal domain of UEV-3, but were hindered by self-activation of the N-terminal expression construct, and were not able to observe strong interactions between either domain alone and PMK-3 (Figure 6A). We then asked if this protein interaction might play roles in the localization or abundance of each protein. We generated transgenic animals expressing functional PMK-3::GFP or UEV-3::GFP in neurons. Both tagged

proteins show ubiquitous expression in cytosol and nucleus (Figure 6B,C).

When each transgene was crossed into *pmk-3* or *uev-3* mutants, we did not

observe major differences in the localization pattern or expression level of

either transgene. As the transgenes likely caused overexpression of the

reporter proteins, it remains possible that subtle changes might have eluded

our detection. However, overexpression of *pmk-3(+)* in *uev-3*; *rpm-1* mutants

does not cause any detectable effects, nor does the overexpression of *uev-3(+)* in *pmk-3; rpm-1* mutants (data not shown). Together with the genetic

epistasis analyses, these data suggest that UEV-3 and PMK-3 could be

obligatory functional partners.

DISCUSSION

The conserved DLK kinases have recently emerged as a key regulator

of axon and synapse development in the nervous systems of both vertebrates

and invertebrates (Po et al., 2010). The mechanistic dissection of the DLK

signal transduction cascade has only just begun. In this study, we identified

and characterized a new member of the DLK-1 kinase pathway, *uev-3*, a

previously uncharacterized ubiquitin conjugating enzyme/E2 variant. Like

other MAPKs known to function in the DLK-1 pathway, loss of function of *uev-3* on its own is grossly wild type, but shows specific suppression of *rpm-1* in

axon termination and synapse formation phenotypes. Our genetic epistasis

studies reveal that *uev-3* acts in the DLK-1 MAPK pathway, downstream of *mkk-4* and upstream of *mak-2*. Based on our studies of UEV-3 protein and its tentative binding interactions with PMK-3, we propose that UEV-3 may act as a co-factor for PMK-3, for example, to modulate PMK-3 activation or to recognize substrates, in fine-tuning the DLK-1 signal transduction cascade.

A ubiquitin conjugating enzyme variant could provide an additional means for pathway regulation and specificity by delineating the targets of the pathway. *C. elegans* has three closely-related p38 MAP kinases that appear to be ubiquitously expressed (Berman et al., 2001). The function of UEV-3 may be to provide specificity for PMK-3 in the DLK-1 MAPK pathway during synaptogenesis and axon termination in neurons. Through the UEV-3 and PMK-3 interaction, substrates important for these processes may be selectively activated. Despite substantial efforts, we have not yet been able to directly test the contribution of UEV-3 in the activation of MAK-2, because of the lack of reagents to detect phosphorylated MAK-2 *in vivo*. However, the idea that UEV-3 could help PMK-3 to affect kinase activation, such as that of MAK-2, would be similar to those revealed by the role of Uev1/Ubc13 in TAK1 kinase activation in the IkK pathway (Deng et al., 2000; Wang et al., 2001).

The transgenic chimera studies suggest that despite the sequence divergency of the UEV domain, UEV-3 likely functions in a manner similar to canonical UEV proteins. Although our studies fail to identify a cognate E2

ubiquitin conjugating enzyme for UEV-3, the possibility that UEV-3 has a

cognate E2 remains. Additional experiments and reagents will be required to

test the remaining UBC genes in *C. elegans*. Our domain-swapping

transgenic studies further hint at roles of the extended N- and C-terminal

domains in UEV-3 in additional regulation of the activity of the UEV domain.

This is consistent with a study in which the N-terminal extension of human

Uev1B was shown to inhibit activity of this isoform when expressed in

Saccharomyces cerevisiae (Andersen et al., 2005)

Finally, an intriguing possibility would be that UEV-3 may be functioning

on its own, and may help add additional regulation in the RPM-1 pathway. It is

well established that the UEV protein Tsg101/Vps23 acts in the endocytic

pathway to bind ubiquitinated proteins and remove them from the membrane

(Katzmann et al., 2002). The endosomal sorting complex required for

transport (ESCRT-1) contains Vps23 and two other Vps proteins necessary for

recognizing and sorting cargo endocytosed at the plasma membrane. Vps23

binds ubiquitin conjugated to proteins at the plasma membrane and together

with the ESCRT-II and -III complexes, target proteins are sorted through

multivesicular bodies in the endosomal pathway. The RPM-1 pathway has

previously been connected to vesicular biogenesis through the biochemical

interaction between RPM-1 and GLO-4 (Grill et al., 2007). A related possibility

is that UEV-3 may provide crosstalk between the GLO-4 and DLK-1 pathways

by binding ubiquitinated proteins through its UEV domain and acting in the endosomal pathway. Potential future directions would be to identify UEV-3 interacting proteins to aid in further elucidating UEV-3's mechanism in axon termination and synapse formation.

Chapter 1, in full, has been submitted for publication of the material as it may appear in *Genetics*. The dissertation author was the primary investigator and author of this paper. The work could not have been done without the initiating work and contributions of Dr. Katsunori Nakata with the support of Dr. Ich N. Maruyama. Dong Yan also contributed significant experiments and critical discussion to this manuscript.

CONCLUSION AND FUTURE DIRECTIONS

An important question that future experiments should address is the

nature of PMK-3 and UEV-3 interaction and output of this interaction. The

experiments must be designed in being important for discerning whether UEV-

3 activity in synapse formation is more related to an endosomal function,

kinase activation, or another mechanism. One hint that UEV-3 may act similar

to UEV protein Tsg101/Vps23 is that Tsg101 interacts with one of its substrate

proteins, p6, via a P-T/S-AP motif (Garrus et al., 2001). PMK-3 contains a

PSAP motif in its N-terminal region. One experiment could test whether this

motif is important for the interaction between UEV-3 and PMK-3 by mutating

the motif and testing for interaction between UEV-3 and PMK-3 via yeast two-

hybrid.

Alternatively, UEV-3 may be aiding in the activation of PMK-3 or in

specifying PMK-3 substrates. One way that UEV proteins have been involved

in activation of kinases is in the NFκB pathway (Skaug et al., 2009). TAB-2

and TAB-3 recognize elongated K63 chains generated by partners Uev1 and

Ubc13, ultimately resulting in the activation of kinase Tak1. Experiments

testing whether UEV-3 is associated with ubiquitin chains and which ubiquitin

the chains are elongated at will be important in advancing the understanding

of UEV-3 function in synapse formation. UEV-3 and PMK-3 do not seem to be

inter-dependent for their localizations and over-expression of either protein

does not compensate for a loss of the other. Perhaps UEV-3 interacts with PMK-3 in its inactive state to ensure that the appropriate targets downstream of PMK-3 are activated. One of the known substrates downstream of PMK-3 is MAK-2, so the role of UEV-3 can be tested by looking at MAK-2 activity in the absence of UEV-3. Phospho-specific antibodies for MAK-2 orthologs are available and have been tested, but results were inconclusive and need to be repeated before further conclusions are made.

Biochemical approaches such as co-immunoprecipitation and mass spectroscopy may be useful in identifying other potential targets downstream of PMK-3 that UEV-3 may be selecting. Epitope-tagged UEV-3 could be used to isolate UEV-3 binding proteins and identify these proteins using mass spectroscopy. Proteins that may be isolated out of this experiment could be an active ubiquitin conjugating enzyme protein and PMK-3 could serve as a positive control for UEV-3 interacting proteins. Another approach might be to try and identify PMK-3 interacting proteins both in the presence and absence of UEV-3 to determine which proteins only interact PMK-3 in the presence of UEV-3.

The possibility that UEV-3 is involved in endosomal sorting is interesting based on another known pathway downstream of RPM-1 that regulates vesicle biogenesis. It would be interesting if UEV-3 provided crosstalk to the GLO-4/GLO-1 pathway and in this way regulates synaptic

vesicle biogenesis or endosomal sorting. Genetic analysis with *uev-3; glo-4* mutants was done and resulted in animals whose phenotype was not any more severe than *glo-4* alone (data not shown). Perhaps the interaction between UEV-3 and GLO-4 pathway is more complex or involves a protein that has yet to be identified.

UEV-3 adds a level of regulation to the DLK-1 pathway in synapse formation and axon termination that is not completely understood at this juncture. Learning more about how PMK-3 and UEV-3 interact and the nature of this interaction will be important for understanding the importance of UEV-3 in these developmental processes.

APPENDIX A: ADDITIONAL UEV-3 EXPERIMENTS

Chapter 1 appears as it was submitted for publication in *Genetics* and described the identification and characterization of *uev-3*, a novel *rpm-1* suppressor. Experiments that were not included in the submitted work will be described in this appendix.

Using epistasis analysis with gain of function *mkk-4*, *uev-3* function was placed downstream of *mkk-4* (Figure 4). Using a gain of function *mak-2*, *uev-3* was placed upstream of *mak-2* based on *uev-3* mutants inability to suppress *mak-2* gain of function phenotypes (Figure 4). qRT-PCR of *cebp-1* mRNA levels in *uev-3* mutants confirmed that *uev-3* acts upstream of *cebp-1* within the DLK-1 MAPK pathway; *uev-3* could also suppress the increase in *cebp-1* transcript levels resulting from *rpm-1* mutants (Figure 4). Another experiment that tested whether the absence of *uev-3* affected levels of MAK-2 and CEBP-1 was to analyze levels of GFP tagged proteins in *uev-3* mutants. Both *mak-2* and *cebp-1* were fused with GFP at the N-terminus (Yan et al., 2009) and visualized in both wild type and *uev-3* mutants. *cebp-1* retained its full 3'UTR in these experiments. Images were captured on confocal microscope and then analyzed using Metamorph. Total cell body fluorescence was measured by tracing the outline of the cell body, subtracting out the background fluorescence and converting to arbitrary units of relative fluorescence. Wild type and *uev-3* mutants were then compared for both GFP-MAK-2(full 3' UTR)

and GFP-CEBP-1 (Figure 7). In a *uev-3* background, levels of GFP-CEBP-1 are decreased compared to wild type, similar to the qRT-PCR results. GFP-MAK-2 levels, however, were unaffected in *uev-3* mutants. It could be that *cebp-1* transcript levels are affected when the MAPK cascade is altered, thus affecting CEBP-1 protein; whereas *mak-2* transcripts are not affected by MAPK pathway signals.

Another approach to determine whether UEV-3 acts up- or downstream of PMK-3 was to create a background in which PMK-3 was constitutively activated and resulted in a gain of function phenotype. Previous work had identified key residues within mammalian p38 for creating an activating mutation, which would disrupt the hydrophobic core (Diskin et al., 2004; Diskin et al., 2007). The corresponding residue in *C. elegans pmk-3* is an aspartic acid at position 281. In order to create the activating mutation, this residue must be converted into an alanine, D281A. Previously, Dr. Katsunori Nakata had created a PMK-3 expression vector containing an E278A mutation, resulting in minimal to moderate effects in motor neuron synapses (data not shown). Dr. Nakata's vector was used as a base vector for creating the additional D281A mutation by site directed mutagenesis. The resulting pan-neuronal expression vector was injected into *muIs32* animals and tested for any gain of function defects. Two separate transgenic animals were isolated from multiple rounds of injection: *juEx1969* and *juEx2308*. In a wild type

background, these animals had either 75% or 37.8% PLM overshoot defect for *juEx1969* and *juEx2308*, respectively (Figure 8). *juEx1969* was tested in a *pmk-3(ju485)* background to determine whether this would create a stronger gain of function phenotype. This did not seem to be the case, so the transgene was crossed into various backgrounds to test whether known molecules up- or downstream of *pmk-3* could suppress the overshooting gain of function phenotype. Mutant backgrounds of downstream molecules, *mak-2(ok2394)* and *cebp-1(ju659),* were able to suppress the gain of function defects in *juEx1969* background. However, upstream molecule *dlk-1(ju476)* was also able to suppress *juEx1969* gain of function defects to degree (57.1% PLM overshoot defects). This data left the result of *uev-3(ju639)* suppressing *juEx1969* PLM overshooting defects as inconclusive.

In the case of transgenic line *juEx2308*, the defects that were observed were not suppressed in upstream protein MKK-4, but downstream molecule CEBP-1 was also unable to suppress these defects. Given that *juEx2308* does not give reliable results with the appropriate controls, the *uev-3* result is not valid. The *pmk-3* gain of function experiments were therefore not successful in further refining the position of *uev-3* with respect to *pmk-3* in the DLK-1 MAPK pathway. The conclusion from yeast two-hybrid data mentioned in Chapter 1 is that UEV-3 and PMK-3 physically interact, which perhaps means that UEV-3 and PMK-3 function at the same level within the MAPK pathway.

To address whether UEV-3 acts with an E2/UBC partner, the available *ubc* mutants were tested for *rpm-1* suppression (mentioned in Chapter 1 as data not shown). From 22 annotated *ubc* genes, five had available mutations to test. *ubc-9, 13, 16, 24, 25* were all tested in *muIs32; rpm-1* background. There were two different alleles available for both *ubc-13* and *ubc-16* that were tested. None of the tested mutants were able to suppress *rpm-1* defects to a significant degree, suggesting that none of the five genes tested is the UBC partner of UEV-3. The possibility remains that UEV-3 may not have a UBC partner, or that the experiments using double mutant analysis, RNAi analysis, and yeast two-hybrid assay may not be good readouts for this interaction.

APPENDIX B: MAPPING ADDITIONAL RPM-1 SUPPRESSORS

ju600 IS A NOVEL *rpm-1* SUPPRESSOR

ju600 was isolated in a mutagenesis screen as previously described (Nakata et al., 2005) using the small, uncoordinated *syd-1; ju44; juIs1* animals and looking for suppression of the small, uncoordinated phenotype. *ju600* was initially identified as a novel suppressor of *rpm-1* when non-complementation tests were carried out against *dlk-1, mkk-4* and *pmk-3*. *ju600* was backcrossed to N2 strain twice before carrying out non-complementation tests, and a third time before continuing with mapping.

The initial non-complementation test results were confirmed again using the same test strains, in addition to a non-complementation test against novel suppressor *uev-3*. All of the non-complementation test strains complemented *ju600* in suppressing the small and uncoordinated phenotype, therefore the *ju600* lesion is not in any of these genes. Non-complementation results for *uev-3* were confirmed by sequencing the exon and intron regions of *uev-3*. No lesions in *uev-3* were identified. *ju600; ju44* was generated for the non-complementation crosses. Non-complementation tests against these suppressors and *ju600* were carried out and none of these showed results consistent with being in the same gene as *ju600*. Non-complementation test with *glr-1* (Hart et al., 1995; Maricq et al., 1995) was also tested after mapping

results indicated *ju600* may have been in the *glr-1* region. *ju600*

complemented *glr-1* and confirmed that the *ju600* lesion is not in *glr-1*.

MAPPING *ju600*

Single nucleotide polymorphisms (SNPs) that result in restriction

enzyme recognition sites (snip-SNPs) were used to map *ju600* against the

natural isolate CB4856 (Wicks et al., 2001). SNPs that can be digested with

DraI from the left and right arm of each chromosome (I-V and X) were selected

(Davis et al., 2005) to identify linkage to the general region containing *ju600.*

CB4856 males were mated to *ju600; ju82; ju44; juIs1* and many F1 cross-

progeny were selected and allowed to self. Small, uncoordinated animals were

picked in the F2 generation in which a certain percent would contain the

suppressor as heterozygous. In the F3 generation, animals resembling *ju600*

with suppressed small, uncoordinated phenotype were selected and these

were kept as recombinants for mapping analysis.

As the suppressor *ju600* was selected for in the crosses, the N2 pattern

of *DraI* digestion would indicate potential linkage to that chromosome.

Fourteen recombinants were used to look for linkage to a chromosomal arm

(Table 4). Because both *syd-1* and *rpm-1* mutations must be maintained in the

strain in order to see suppressor phenotype, N2 pattern is also obvious at

these chromosomal positions. *syd-1* is located at II+0.5 and *rpm-1* is located

at V+1.6. The initial experiment showed linkage to Chromosome III and an

additional twenty-eight recombinants were tested for the same SNPs before selecting this region to narrow further. Ultimately, a total of fifty-three recombinants were used to map linkage for *ju600.* Sixty-three recombinants mapped *ju600* to the region between III-4.12 and III+0.5 (Table 5). The most informative recombinants were backcrossed and reisolated to ensure that they were true recombinants.

A ubiquitin conjugating enzyme, *ubc-18,* is located on Chromosome III within the region that *ju600* was mapped to. The exon and intron regions for this gene were sequenced and no lesions were identified. To obtain additional information about the location of the *ju600* lesion, three factor crosses were used with *lon-1 unc-36* animals. *lon-1* is located at III-1.64 and *unc-36* is located at III-0.3. Using *muIs32; ju44* animals to cross to *lon-1 unc-36*, the resulting males were then crossed to *muIs32; ju600; ju44* and two populations of animals were selected: long, non-uncoordinated and non-long, uncoordinated worms. Animals were then genotyped for *ju44* and scored visually for *rpm-1* suppression to ensure *ju600* was homozygous. Three long, non-uncoordinated worms were isolated and determined to be homozygous for *ju44.* Ideally, non-long, uncoordinated animals would have been isolated in this process as well, giving more information about where *ju600* is located based on the ratios of the two phenotypes. *lon-1 ju600* was also used for non-complementation tests for genes of interest that did not have observable

phenotypes. For example, *twk-7* was a gene of interest located within the mapped region. Results from these crosses cannot be trusted because a later backcross of the *muIs32; lon-1 ju600; ju44* strain resulted in segregation of *ju600* and *lon-1* such that the two are not linked.

Another approach used to assist in finding the *ju600* locus was the deficiency test using *nDf20.* The strain containing *nDf20* is *nDf20/sma-2 unc-32* where *nDf20* covers the region III-0.56 to III-0.13*. sma-2* is located at III-0.06 and *unc-32* is at III. Deficiency tests take advantage of the large region missing in these animals and usually result in a sterile or obvious phenotype when the deficiency is homozygous. The mutation of interest, *ju600*, was crossed to the *nDf20/sma-2 unc-32* strain and any F1s that were isolated that segregated *sma-2 unc-32* animals were tossed. In the F2s from animals not throwing *sma-2 unc-32* animals, the animals would either be *nDf20/ju600* or *ju600* homozygous because *nDf20* homozygotes are sterile. If the *nDf20/ju600* animals are also able to suppress *ju44*, this suggests that the gene with the *ju600* lesion is contained within the *nDf20* region. Two repeats of *nDf20* experiments showed that *ju600* is not within the *nDf20* region. The strain carrying *lon-1 ju600* was also used to cross to *nDf20* and yielded the same results.

The region containing *ju600* was narrowed to the III-0.38 to III-0.134 region and twenty-one cosmids covering the region were requested to test for

rescue activity. Initially the following cosmids were ordered to test rescue of

ju600 in *muIs32; ju600; ju44* by injection: C14B9 D2007 C50C3 C30A5 C02F5

F09G8 F10E9 ZC262 R05D3 ZK353 ZK1236 C30C11 F42H10 C04D8 ZC21

C02D5 C06E1 C13G5 F22B7 B0523. Eighteen cosmids could be recovered

and after enzyme digest showed the correct size. Cosmids were separated

into batches and injected, looking for stable lines and then checking *muIs32*

phenotype for rescue activity. Simultaneous mapping eliminated some regions

containing cosmids that were subsequently not used for injection. At least

three stable transgenic lines per cosmid injection mix were analyzed for *ju44*

suppression. One injection mix attempted (called injection mix 2) included

C30C11, ZK353, R05D3, D10C7, F42H10, ZC262, ZK1236, and F22B7.

Three transgenic lines were isolated from this injection and none of the lines

were able to rescue *ju600* suppression. The next cosmid mix (injection mix 3)

included K10C7, F22B7 and did not contain rescue activity in any of the lines

tested. Another mix (injection mix 4) including C30C11, ZK353, R05D3,

F42H10, ZC262 and ZK1236 was attempted, without any rescue of

suppression.

ju600 SUPPRESSES *rpm-1* MECHANOSENSORY NEURON DEFECTS

   rpm-1 mutants have previously been shown to have defects in

mechanosensory neuron termination (Schaefer et al., 2000). Suppressors of

rpm-1, therefore, have been shown to also suppress the axon termination

defect in mechanosensory neurons ALM and PLM (Chapter 1, (Schaefer et al., 2000)). To test the extent to which *ju600* suppresses the mechanosensory neuron defects of *rpm-1*, the *ju600; ju44* strain was examined in a *muIs32 [Pmec-7-GFP]* background. *ju600* can suppress ALM hooking defects from 61.02% to 16.95%, while PLM hooking is suppressed 79.66% to 1.69%. PLM synaptic branch defects are also suppressed from 41.38% to 18.64%. The *lon-1 ju600; ju44* strain was also generated in a *muIs32* background and scored for suppression of *rpm-1* defects. ALM hooking was suppressed to 5.17%, PLM hooking to 3.45%, and PLM synaptic branch defects to 29.82% in *muIs32; lon-1 ju600; ju44* animals. *muIs32; lon-1; ju44* animals were also analyzed and showed very similar defects to *muIs32; ju44* animals with 51.92% ALM hooking, 80.77% PLM hooking and 30.77% PLM synaptic branch defects.

FUTURE OF *ju600*

Recently, mapping of *ju600* has been attempted once more using more thorough approaches, such as whole genome sequencing (Sarin et al., 2008). Based on preliminary evidence after mapping recombinants using a *muIs32; ju600; rpm-1(ju44); syd-2(ju37)* strain, results indicate the *ju600* suppression activity is due to lesions in two locations: one near Chromosome III+0, the other is on Chromosome I. In retrospect, this result explains the difficulty in rescuing *ju600* using only cosmids covering regions on Chromosome III, along

with questionable results when using three-factor mapping and the linked

strain *ju600 lon-1.*

PRELIMINARY MAPPING SUPPRESSORS *ju657, ju660, ju666, ju667*

Other suppressors isolated out of the suppressor mutagenesis screens

were identified as novel suppressors by non-complementation tests against

the known *rpm-1* suppressors. Novel suppressors from the *syd-2(ju37); rpm-*

1(ju44) were *ju657* and *ju660.* The novel suppressors from the *syd-1(ju82);*

rpm-1(ju44) screen were *ju666* and *ju667*. *ju666* and *ju667* were identified as

non-allelic with *ju600* after non-complementation tests using *ju600; ju44*. *ju667*

non-complementation test results with the MAPK pathway members were

reconfirmed and tested with *uev-3*. The *uev-3* non-complementation test result

was further confirmed by sequencing the exon and intron regions; there were

no lesions identified. CB4856 *DraI* snip-SNP mapping was used to determine

preliminary results for chromosomal arm linkage (Table 4). Additional

recombinants were isolated to further narrow arm linkage for *ju667* (Table 4).

Using CB4856 DraI snip-SNP mapping, *ju660* was mapped using F2

recombinants such that the F2 small and uncoordinated double mutants were

isolated and then used to map for the absence of the suppressor mutation.

These recombinants would therefore contain CB4856 at the suppressor region

instead of N2. Between 11 and 86 recombinants were mapped for various

points on each of the six chromosomes. Specifically, Chromosome I contained

a large number of CB4856 patterns, especially at I+12 and I+15.5 with 73 and 86 recombinants, respectively (Table 4). Because *dlk-1* is located at I+13.62, *ju660* was sequenced for lesions in the exon and intron regions. *ju660* defines a G to A transition at nucleotide 736, which causes an aspartic acid (D) to asparagine (N) change at position 246 in the kinase domain.

ju657 was also mapped for F2 recombinants and initial arm linkage suggested that the lesion may be on Chromosome I (Table 4), also in the same region as *dlk-1*. However, after sequencing intron and exon regions within *dlk-1*, no lesions were identified.

APPENDIX C: MAPK/UBIQUITIN RNAI SCREEN

With the identification of *uev-3* as a suppressor of *rpm-1* and the

identities of both proteins related to the ubiquitin pathway, the possibility

existed that additional ubiquitin-related proteins might also be in the RPM-1

pathway. As an alternate approach to identifying molecules downstream of

rpm-1, a candidate approach was taken using all the genes currently

annotated in the *C. elegans* genome with any domain or motif related to

"ubiquitin". The function of these genes downstream of RPM-1 was then tested

by inhibiting these genes using RNA interference. RNA interference (RNAi) is

a process by which the translation of mRNA is inhibited by corresponding

double-stranded RNA (dsRNA) as a regulatory mechanism within organisms

(general ref).

Since the advent of RNAi in *C. elegans* (Timmons and Fire, 1998), the

technique has been a robust reverse genetics approach, particularly for genes

with embryonic lethal or other phenotypes that complicate examining or

obtaining mutant alleles. Targeting genes expressed in the nervous system

has prove challenging, as neurons are selectively impervious to RNAi

(Tavernarakis et al., 2000). Attempts to understand more about the RNAi

pathway have led to discoveries of components of the RNAi machinery that,

when mutated, result in sensitivity of RNAi in neurons (Kennedy et al., 2004;

Simmer et al., 2002). *eri-1(mg366)IV* is a mutation in a gene responsible for

negatively regulating RNAi by degrading small interfering RNAs (siRNA),

thereby inhibiting the RNA-induced silencing complex (RISC) (Kennedy et al.,

2004). *rrf-3* is a dsRNA-depending RNA polymerase (RdRP) and this mutant

background has also been shown to increase the effectiveness of RNAi in

neurons (Simmer et al., 2002; Wang and Barr, 2005). *eri-1(mg366); rpm-*

1(ju44); syd-2(ju37) was constructed by Dr. Katsunori Nakata to test

suppression of *rpm-1* by looking for suppression of the small and

uncoordinated phenotype of *rpm-1(ju44); syd-2(ju37)* mutant worms. *eri-1* was

used to additionally sensitize these animals to dsRNA.

Administering dsRNA to worms can be executed in a number of ways

(Wang and Barr, 2005), and with approximately 350 genes to test (Table 6);

the feeding protocol was chosen to test the ubiquitin library. The genes

available in the Ahringer Lab RNAi library were tested in two trials using the

feeding RNAi protocol. Larval stage 4 (L4) animals were placed on the bottom

wells of 6-well plates seeded in duplicate with each test dsRNA-containing

bacteria. Animals were left on original well for 24 hours before they were

moved to the top wells for an additional 3 days. Progeny from the top wells

were then scored for improved movement. Any genes that had even a partial

suppression phenotype were retested to check the phenotype. Control RNAi

strains used included known suppressors *dlk-1, mkk-4,* and *uev-3.*

Although there were genes that looked like partial suppressors in the first trial, repeating these experiments did not replicate initial results. In addition to testing the batch of 361 genes, of the 22 *ubc* genes, 17 available RNAi clones were singled out and tested again when attempting to find the E2 that works with *uev-3* (see also Chapter 1). None of these genes were able to suppress the small, uncoordinated movement phenotype. These genes were also tested in a *muIs32; eri-1(mg366); rpm-1(ju44)* background looking for suppression of the *rpm-1* PLM hooking phenotype. None of the *ubc* genes tested suppressed this phenotype.

PROPOSAL FOR NSF GK-12 PROJECT PUBLICATION

The NSF GK-12 grant provides a unique partnership with local area high school science teachers and graduate students. The relationship provides an opportunity for Fellows to create an inquiry-based curriculum piece based on their own research, while simultaneously practicing science communication skills. The introduction of *Caenorhabditis elegans* into biology classrooms was enthusiastically received; students were engaged in their learning experiences and performed well on tests that covered related concepts.

Over the course of the 2009-2010 academic year, I implemented the following student-centered learning lessons: 1) *C. elegans* was first introduced to students in an activity to stimulate discussion about the soil ecosystem. Students brought their own soil samples into the classroom to isolate *C. elegans* and other "life forms" from the soil. 2) We used *C. elegans* to demonstrate Mendelian ratios in live organisms, since much of my dissertation research is based on genetic analysis. Students receive progeny from genetic crosses between wild type and a visually appealing mutant. They then distinguish the phenotypes and calculate ratios to determine whether a mutant allele is dominant or recessive to wild type. 3) *C. elegans* chemotaxis investigates the function of the nervous system by examining a simple circuit important in olfaction. Students carry out a chemotaxis assay using animals with wild type and mutant responses to odorant attractants almond extract and

buttered popcorn. Overall the partnership and experiments highlight student-driven inquiry and the scientific process as practiced by laboratory scientists.

The work in high school classrooms over the past year can be sustained in high school classrooms if schools have access to some of the inexpensive resources required to maintain *C. elegans*. I intend to work with the NSF GK-12 team at UCSD and teacher partner at Hilltop High School to ensure that these activities are sustained through either publication in an education journal or adoption into the UCSD ScienceBridge Program. Additional work with students participating in ScienceBridge summer programs may result in new activities using *C. elegans* to teach students important concepts in biology.
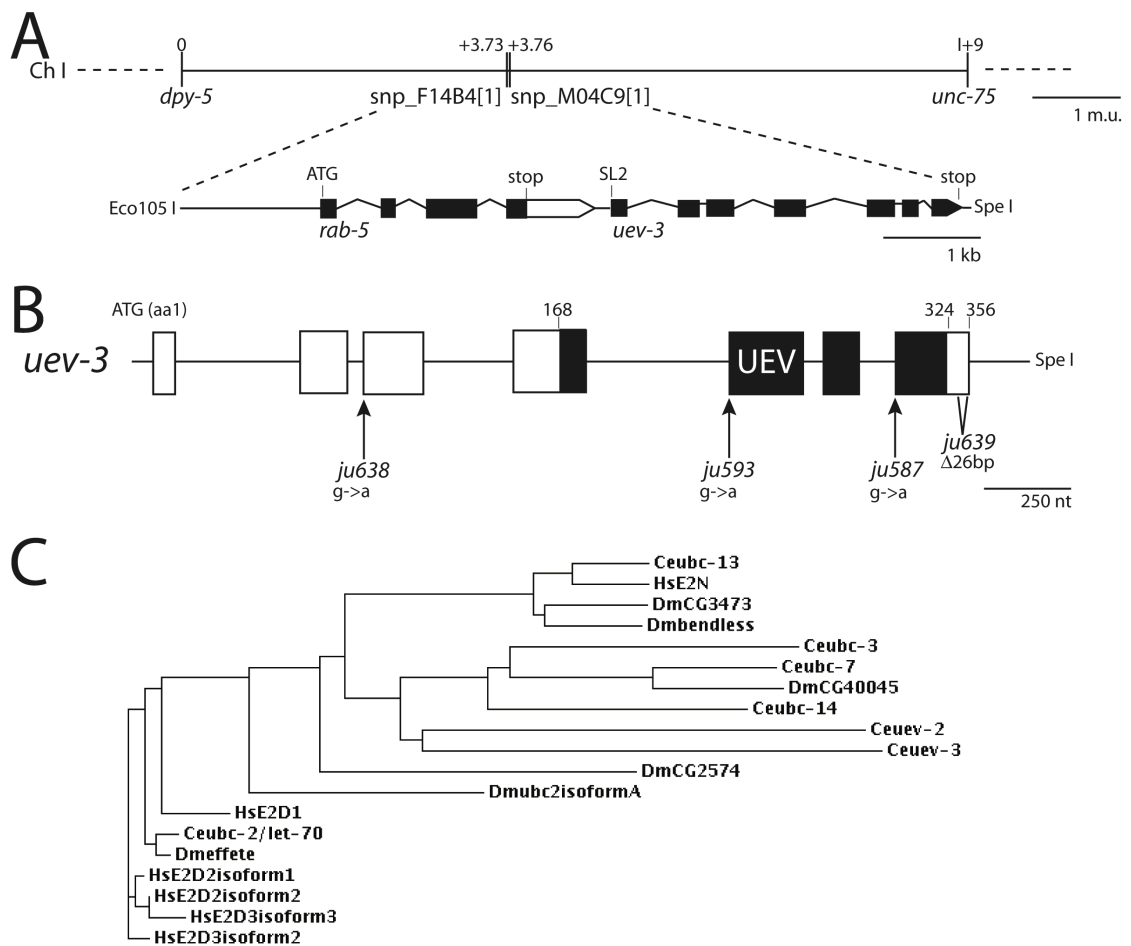
FIGURE 1. *uev-3* is a ubiquitin E2 variant. **A.** The suppressor mutations were mapped to Chromosome I, between +3.73 and +3.76 using single nucleotide polymorphisms. The Eco1051-SpeI genomic fragment from cosmid F26H9 contains the *rab-5* and *uev-3* operon, and fully rescues the suppression of *rpm-1(lf)* by *uev-3* mutations. Black box are coding sequences, white box 3' UTR, and lines, promoter or intronic sequences. **B.** Illustration of *uev-3* gene structure and positions of the mutations. Boxes are exons and black shading marks the UEV domain. **C.** Dendrogram of UEV-3 with close homologs using ClustalW with top six BLAST hit in *C. elegans*, *D. melanogaster*, and *H. sapiens*.

FIGURE 2. *uev-3* suppresses *rpm-1* defects in motor neuron synapse formation and mechanosensory neuron axon termination *A.* Top left schematic illustrates an animal expressing *Punc-25-SNB-1::GFP* (*juIs1*) to visualize presynaptic terminals of the GABAergic neuromuscular junctions. Cell bodies (large gray dots) reside in the ventral cord, and synaptic SNB-1::GFP puncta (small green dots) are present along the ventral and dorsal cords. The epi-fluorescent images below show SNB-1::GFP in the dorsal cords in one-day old adult animals with genotypes as indicated. Scale bar represents 10µm. *rpm-1(ju44)* mutants display irregularly distributed and sized SNB-1::GFP compared to wild type. *uev-3* mutants are indistinguishable from wild type. *rpm-1(ju44); uev-3(ju587)* double mutants show significant suppression of the SNB-1::GFP phenotype. The graph on the right shows the quantification of SNB-1::GFP in the dorsal cord (mean ± SEM). n indicates number of animals scored. Statistics, Student's t test: * $P<0.05$, ** $P<0.01$, *** $P<0.001$, ns = not significant. *B.* Schematic of animal expressing *Pmec-7::GFP* (*muIs32*) to visualize mechanosensory neurons, marking one each of the bilaterally symmetric ALM and PLM neurons. Images below show portion of the ALM and PLM axons, corresponding to the dash-boxed regions. The tip of the animal's nose is indicated with aqua arrows, and ALM and PLM axon termination site is indicated with purple arrows. PLM cell body is in the tail and projects an anterior axon, which terminates just posterior to ALM cell body (red asterisks). ALM axon termination defects occur when the axon tip extends into the tip of the nose and loops back (or hook) as shown for *rpm-1* or *uev-3; rpm-1* as compared to wild type or *uev-3* alone. PLM axon termination defects include two categories: absence of synapse branch or "hook" such that the PLM axon either overextends beyond normal termination site and turns ventrally or turns ventrally before normal termination site. The graph shows the suppression of *rpm-1* by *uev-3* in three categories. n indicates animals scored. Statistics, measured using Fischer Exact Test, comparing the PLM "hook" defects: * $P<0.05$, ** $P<0.01$, *** $P<0.001$, ns = not significant.

A

B

ALM   PLM

wild type

rpm-1

uev-3(ju639)

uev-3(ju639); rpm-1
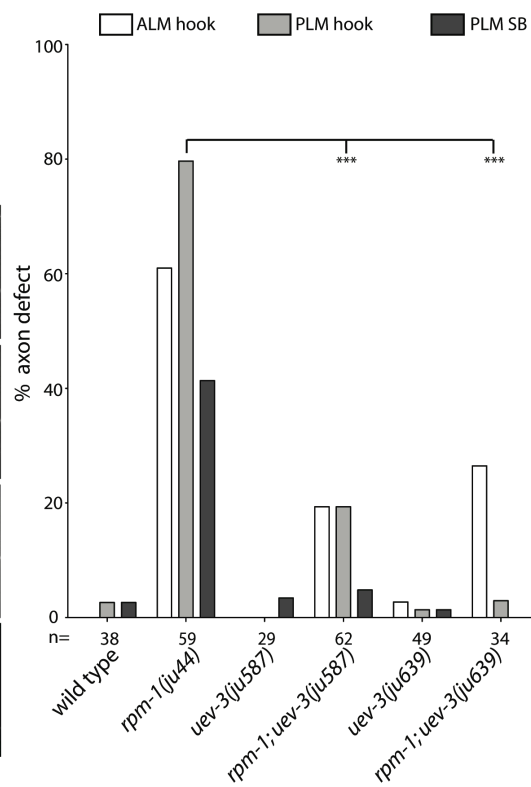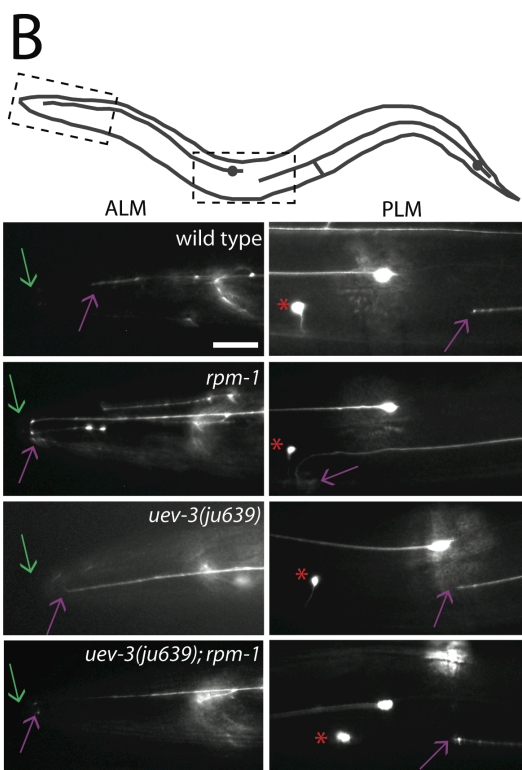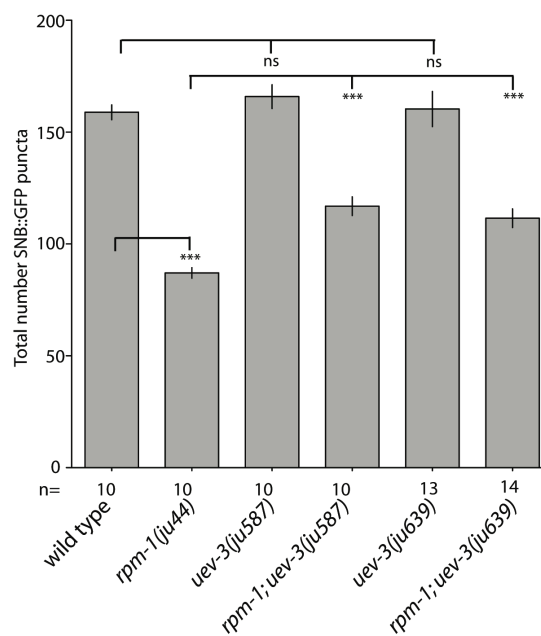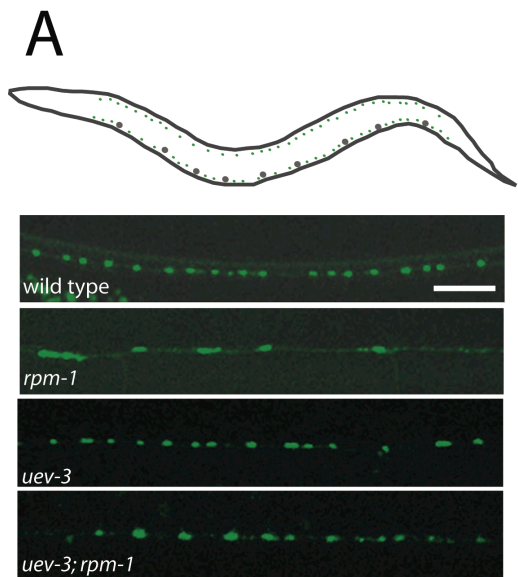
FIGURE 3. UEV-3 functions cell autonomously in presynaptic neurons. ***A.*** Shown is an image of a transgenic animal expressing the 1.8 kb promoter of the operon driven GFP (*ixEx2 [Puev-3-GFP]*). GFP is observed in many tissues (left panel), and in the motor neurons of the ventral cord (white arrows in right panel). ***B.*** Presynaptic expression of UEV-3 rescues the suppression of *rpm-1* by *uev-3* in the GABAergic motor neurons. *Prgef-1*, 3.5kb pan-neural promoter; *Punc-25*, 1.2kb GABAergic motor neuron promoter, and *Pmyo-3*, 1kb body muscle promoter. Quantification of SNB-1::GFP puncta in the dorsal nerve cord of young adults is shown as mean ± SEM; n as indicated. Statistics, Student's *t* test: * $P<0.05$, ** $P<0.01$, *** $P<0.001$, ns = not significant. ***C.*** Cell-autonomous rescue of the suppression of *rpm-1 by* uev-3 in touch neurons driven by the *Pmec-4* promoter. n indicates animals scored. Statistics, Fischer Exact Test, comparing the PLM "hook" defects: * $P<0.05$, ** $P<0.01$, *** $P<0.001$, ns = not significant.

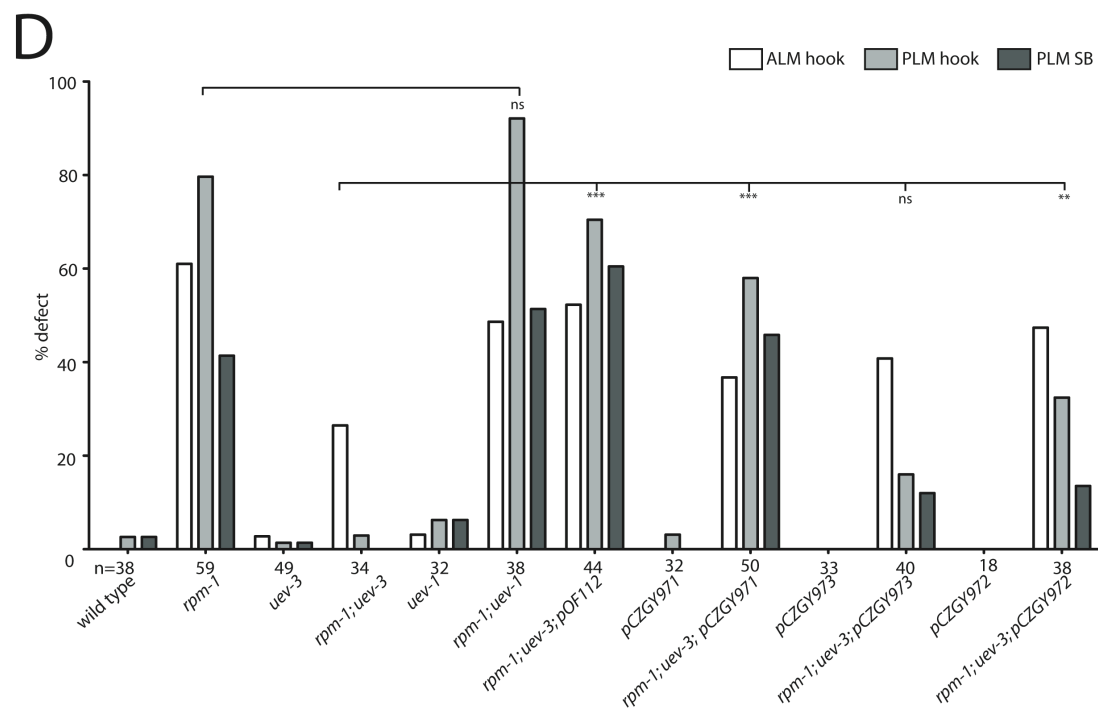A *Poperon-rab-5-uev-3* GFP
   1.8kb
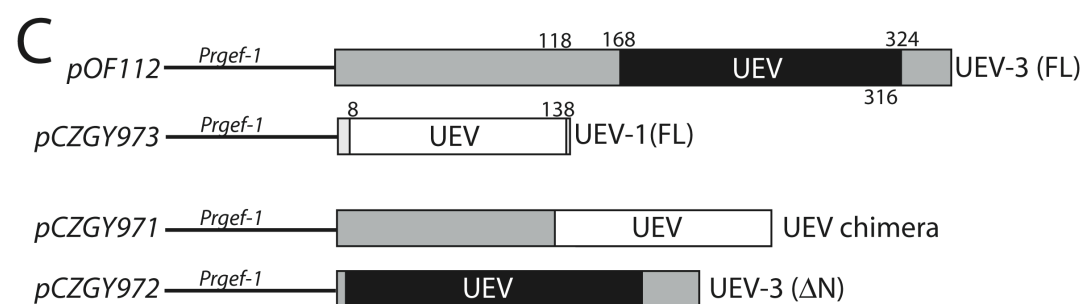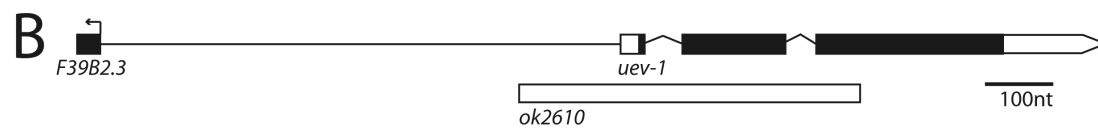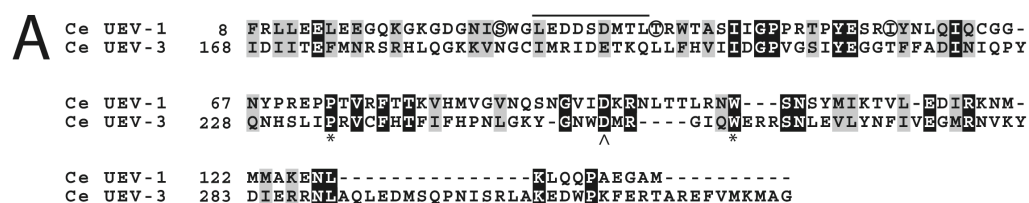
B

C

ALM hook   PLM hook   PLM SB
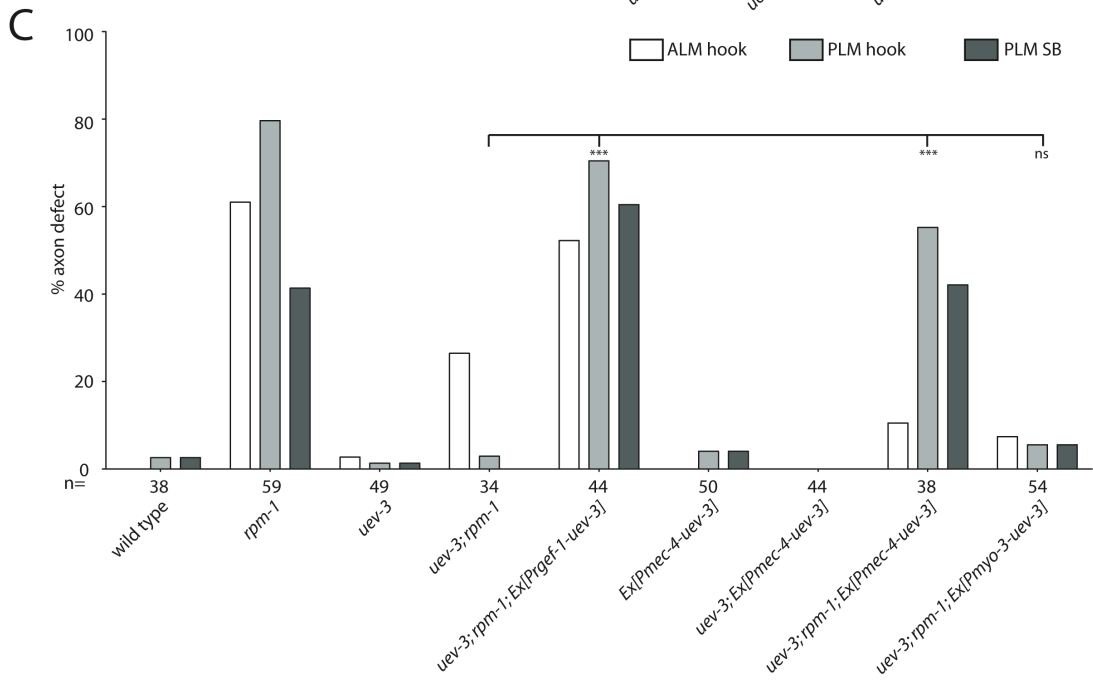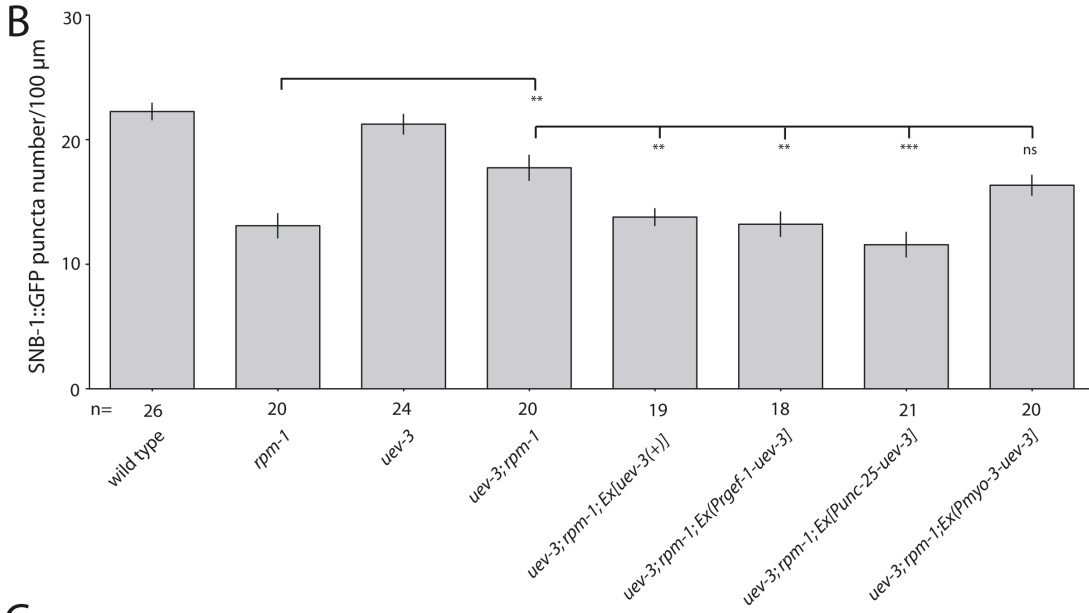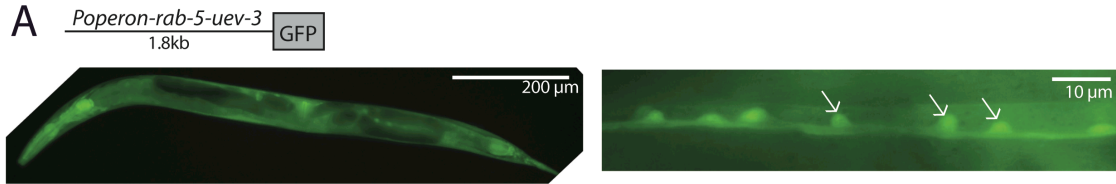
FIGURE 4. *uev-3* acts in the DLK-1 MAPK cascade, downstream of *mkk-4*, and upstream of *mak-2*. **A.** *uev-3(lf)* does not further enhance the suppression of *rpm-1* in the motor neuron synapses by *pmk-3* or *mkk-4*. Numbers are mean ± SEM, n as indicated. Statistics, Student's t test compared with *rpm-1* single mutant: * P<0.05, ** P<0.01, *** P<0.001, ns = not significant. **B.** *uev-3* functions downstream of *mkk-4* MAPKK. Transgenic animals overexpressing wild-type MKK-4 [*mkk-4(++), juEx490*] or expressing the constitutively active version of MKK-4 [*mkk-4(DD), juEx669*] in wild type background display similarly abnormal synaptic patterns (*juIs1*), uncoordinated locomotion, and small body size (left). The phenotypes of both types of transgenes are suppressed by *uev-3(ju587),* and quantitation is shown on the right (mean ± SEM); Student's t test: * P<0.05, ** P<0.01, *** P<0.001, ns = not significant, n as indicated. **C.** *uev-3* acts upstream of *mak-2*. Expression of a phosphomimetic MAK-2(EE) causes gain-of-function effects on neurons such that PLM axon overextends, which is suppressed by *cebp-1*, but not by *uev-3.* n as indicated. Statistics, Fischer Exact Test * P<0.05, ** P<0.01, *** P<0.001, ns = not significant. **D.** *uev-3* acts in the *dlk-1* pathway to regulate levels of *cebp-1* transcripts. Shown are qRT-PCR levels of *cebp-1* mRNAs normalized against *ama-1*. The levels of *cebp-1* in *uev-3* are comparable to that in wild type and *dlk-1*. *uev-3(lf)* also suppresses the elevated levels of *cebp-1* mRNA caused by *rpm-1(lf).* Statistics, Student's t test: * P<0.05, ** P<0.01, *** P<0.001, ns = not significant, n=3.
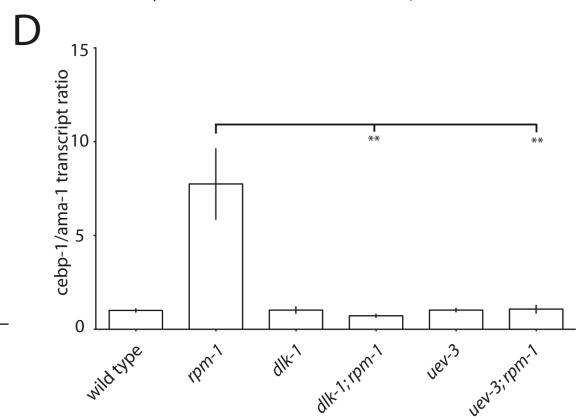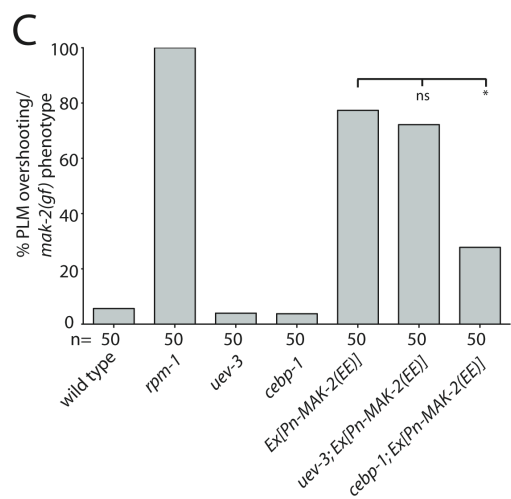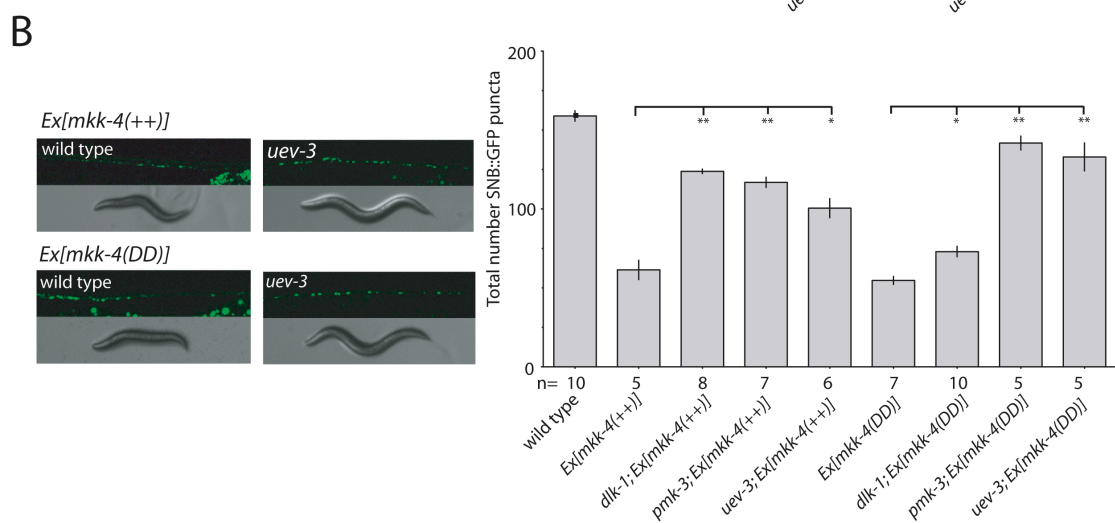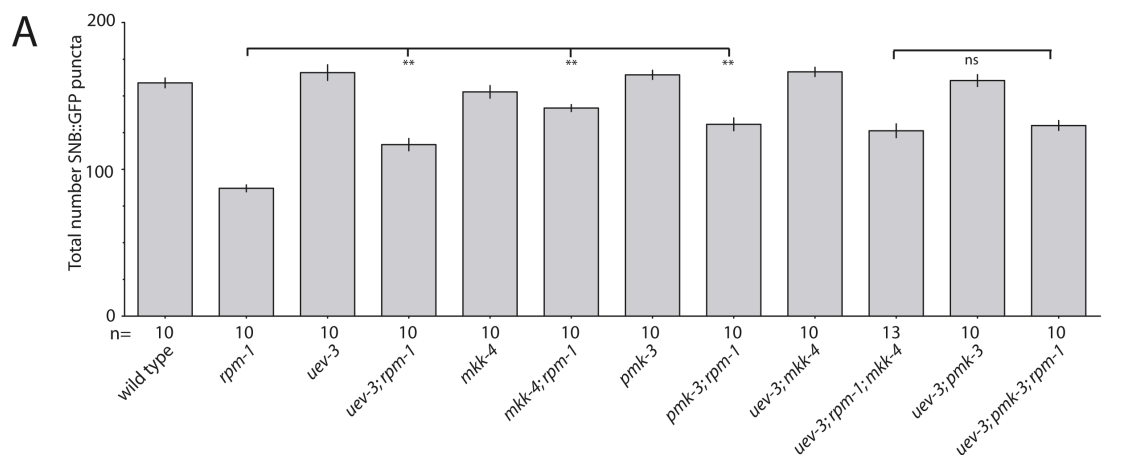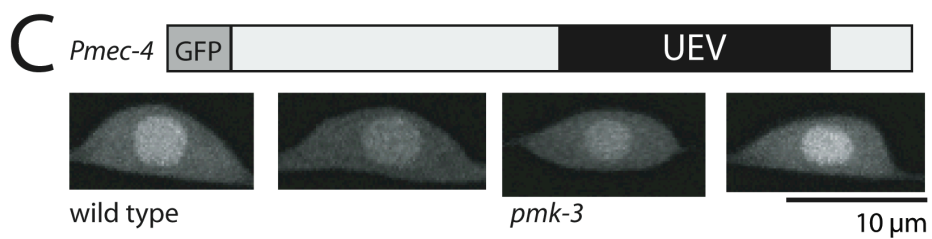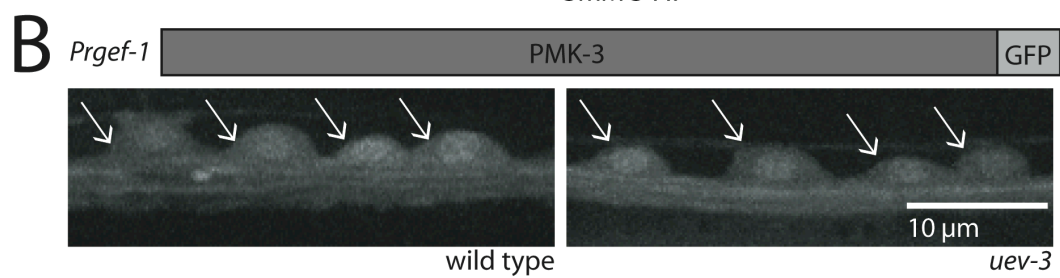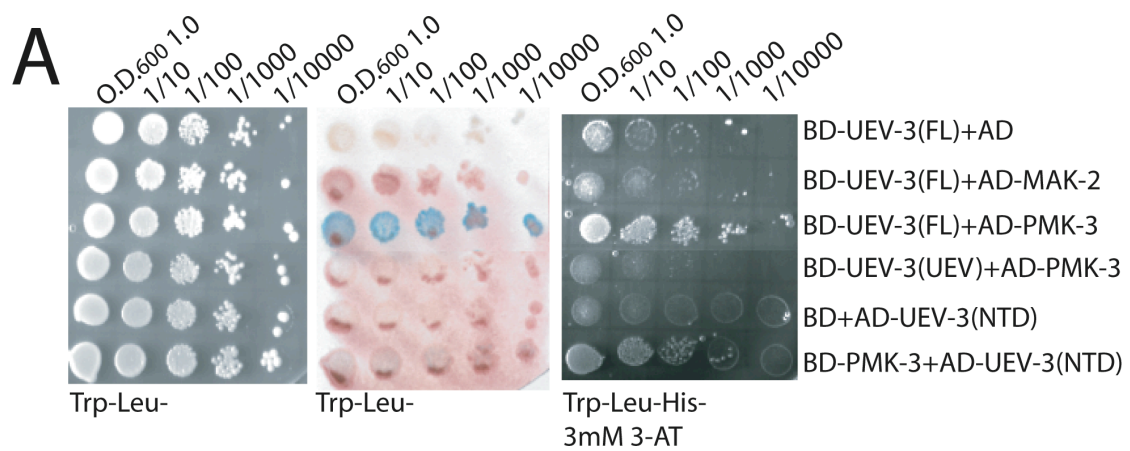
FIGURE 5. UEV-3 likely functions similarly to canonical UEV proteins*. **A.** Alignment of UEV-1 and UEV-3 UEV domains. Black boxes indicate identical residues and grey boxes are similar residues. Asterisk indicates conserved proline and tryptophan residues; caret indicates aspartic acid residue at the position where both UEV proteins lack the active cysteine. Solid line above residues in UEV-1 31-39 indicates the conserved region that would be important for interacting with Ubc13. Circled Ser, Thr and Ile residues have been shown to be on the interface of *S. cerevisiae* Mms2 with ubiquitin, which are not conserved in UEV-3. **B.** Illustration of the *uev-1* gene. *ok2610* deletes 496bp, starting 142bp in the 5' promoter region and ending 69bp into the third exon of *uev-1*, and is most likely a null mutation of *uev-1*. **C.** Schematics of DNA constructs used to assess domain importance in UEV-3. *Prgef-1* pan-neuronal promoter was used to drive all constructs **D.** Quantification of transgenic expression of UEV chimera. UEV domain from UEV-1 into that of UEV-3 is sufficient to relieve suppression of *rpm-1*. Domain dissection experiments show the N-terminus of UEV-3 is important, but not required. *uev-1(lf)* does not suppress *rpm-1(lf)* hooking or synaptic branch defects. 3-13 transgenic lines were scored for each construct, data from a representative line is shown. n as indicated. Statistics, Fischer Exact Test * P<0.05, ** P<0.01, *** P<0.001, ns = not significant.

A

```
Ce UEV-1    8   FRLLEELEEGQKGKGDGNISWGLEDDSDMTLTRWTASIIGPPRTPYESRIYNLQIQCGG-
Ce UEV-3   168  IDIITEFMNRSRHLQGKKVNGCIMRIDETKQLLFHVIIDGPVGSIYEGGTFFADINIQPY

Ce UEV-1   67   NYPREPPTVRFTTKVHMVGVNQSNGVIDKRNLTTLRNW---SNSYMIKTVL-EDIRKNM-
Ce UEV-3   228  QNHSLIPRVCFHTFIFHPNLGKY-GNWDMR----GIQWERRSNLEVLYNFIVEGMRNVKY
                      *                          ^            *

Ce UEV-1   122  MMAKENL---------------KLQQPAEGAM----------
Ce UEV-3   283  DIERRNLAQLEDMSQPNISRLAKEDWPKFERTAREFVMKMAG
```

B

F39B2.3   *uev-1*

ok2610   100nt

C

pOF112   *Prgef-1*   118 168   UEV   324   UEV-3 (FL)   316

pCZGY973   *Prgef-1*   8   UEV   138   UEV-1(FL)

pCZGY971   *Prgef-1*   UEV   UEV chimera

pCZGY972   *Prgef-1*   UEV   UEV-3 (ΔN)

D

ALM hook   PLM hook   PLM SB

% defect

100

80

60

40

20

0

ns   ***   ***   ns   **

n=38   59   49   34   32   38   44   32   50   33   40   18   38

wild type   *rpm-1*   *uev-3*   *rpm-1;uev-3*   *uev-1*   *rpm-1;uev-1*   *rpm-1;uev-3;pOF112*   *pCZGY971*   *rpm-1;uev-3;pCZGY971*   *pCZGY973*   *rpm-1;uev-3;pCZGY973*   *pCZGY972*   *rpm-1;uev-3;pCZGY972*

FIGURE 6. UEV-3 likely binds PMK-3. ***A.*** Yeast two-hybrid interaction assay showing that UEV-3 interacts with PMK-3 but not with MAK-2. Colonies grown to OD600 1.0 and diluted 1:10, 1:100, 1:1000, and 1:10000 and selected on Trp-Leu- plates (left panel). Interactions are tested by lacZ assay (middle panel), and on Trp-Leu-His- plates containing 3mM 3-AT (right panel). UEV-3(FL) indicates full-length UEV-3, UEV-3(UEV) indicates UEV domain only, UEV-3(NTD) indicates N-terminal domain, BD is binding domain and AD is activating domain. ***B.*** Functional PMK-3::GFP (*juEx675 [Prgef-1-PMK-3::GFP]*) in neurons is seen in cytoplasmic and nuclear compartments in wild type, and is unaltered in *uev-3(ju587)* background. Arrows indicate neurons in the ventral cord. ***C.*** Functional UEV-3::GFP in mechanosensory neurons *[juEx2118 Pmec-4-GFP::UEV-3]* localizes to cytoplasm and nucleus, and is unaltered in *pmk-3* mutant background.

A

O.D.600 1.0 1/10 1/100 1/1000 1/10000　　O.D.600 1.0 1/10 1/100 1/1000 1/10000　　O.D.600 1.0 1/10 1/100 1/1000 1/10000

BD-UEV-3(FL)+AD

BD-UEV-3(FL)+AD-MAK-2

BD-UEV-3(FL)+AD-PMK-3

BD-UEV-3(UEV)+AD-PMK-3

BD+AD-UEV-3(NTD)

BD-PMK-3+AD-UEV-3(NTD)

Trp-Leu-　　　　　Trp-Leu-　　　　　Trp-Leu-His-
　　　　　　　　　　　　　　　　　　3mM 3-AT

B

Prgef-1　| PMK-3 | GFP |

wild type　　　　　　　　　　　　　　　　10 μm　　*uev-3*

C

Pmec-4　| GFP | | UEV | |

wild type　　　　　　　　*pmk-3*　　　　10 μm

FIGURE 7. Sequence alignment surrounding the active region in Ubc proteins showing homology between *H. sapiens*, *C. elegans*, and *D. melanogaster* from C. Exact matches are shaded in black, similar residues are shaded in grey. Asterisk denotes where UEV-3 lacks the critical cysteine residue. The Ubc folding motif, HPN/HCN, is noted by an underline.
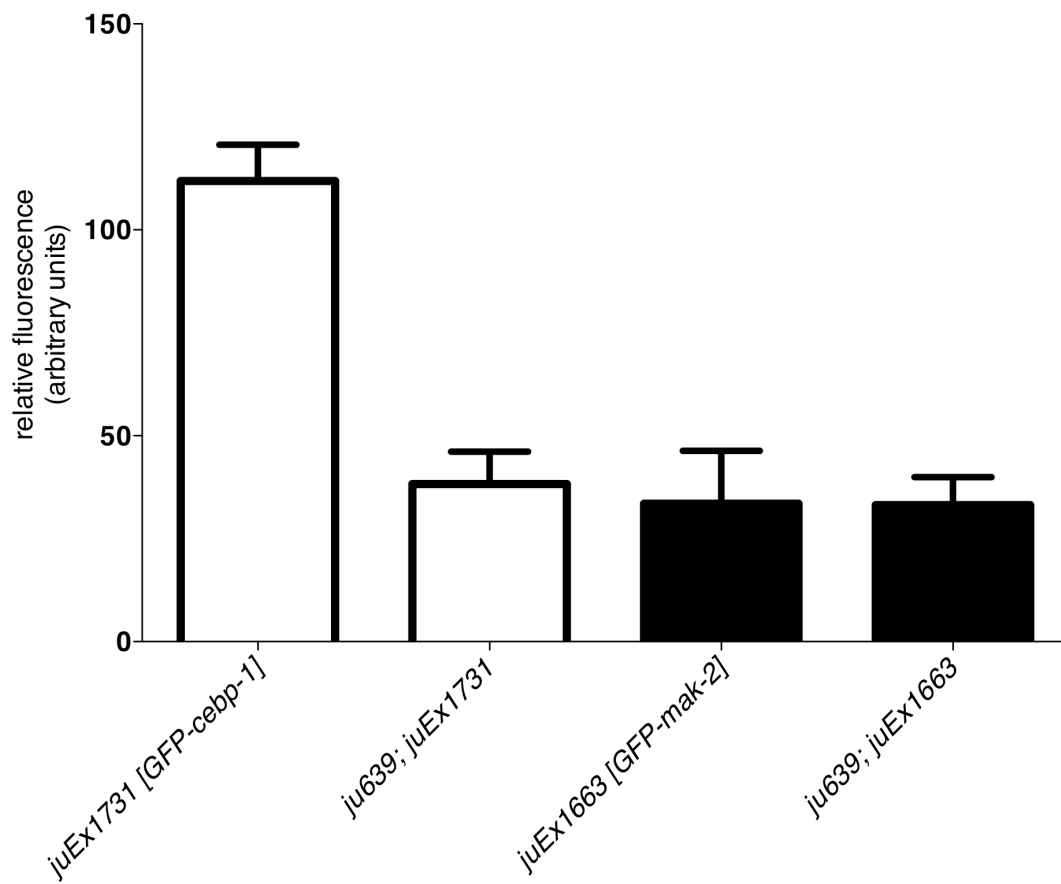
FIGURE 8. Expression of MAK-2 and CEBP-1 in *uev-3* mutant background.
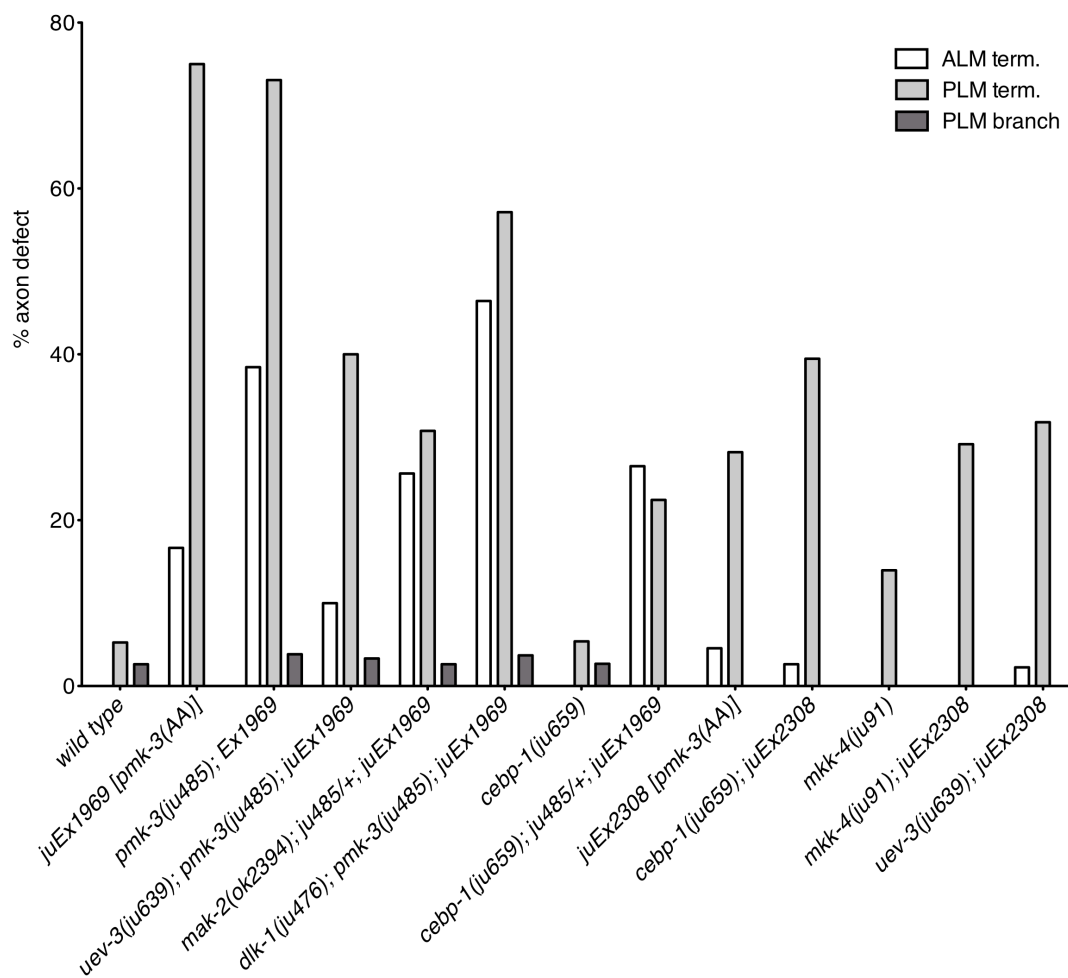
FIGURE 9. Epistasis analysis using gain of function *pmk-3*.
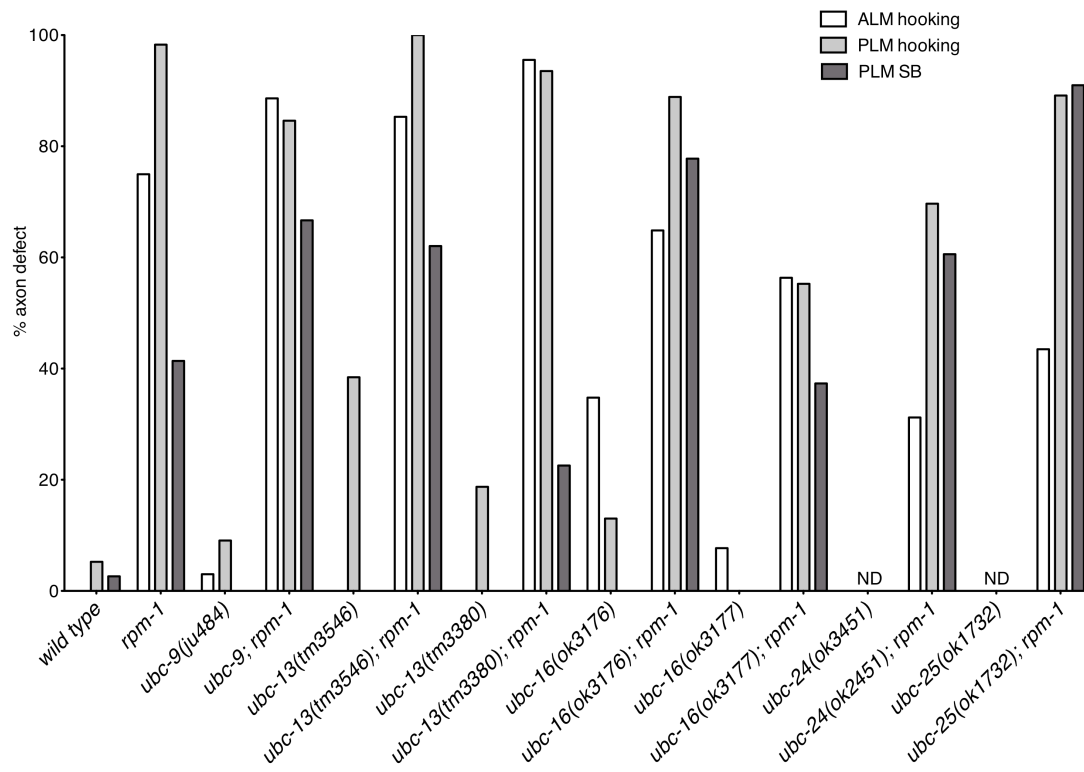
FIGURE 10. *ubc* mutants do not suppress *rpm-1* axon termination defects. At least 20 animals per genotype were scored. ND = no data.
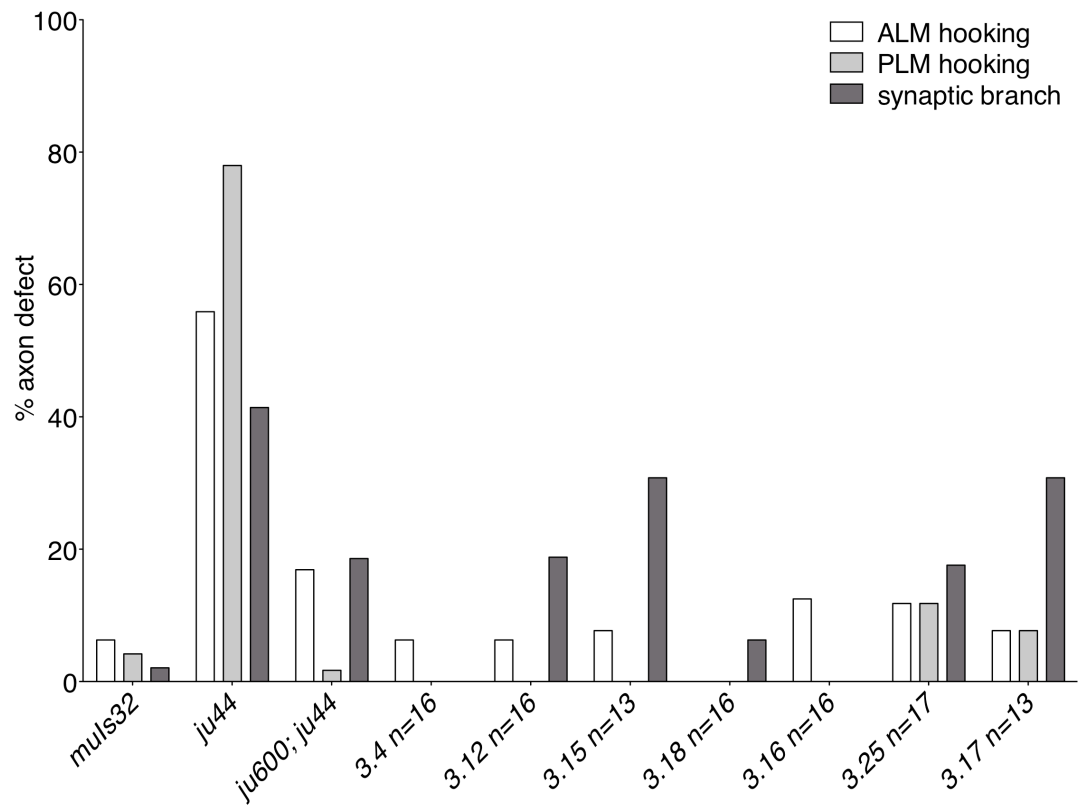
FIGURE 11. Cosmid mix 3 does not rescue *ju600*. Lines are indicated by 3.x, followed by n.
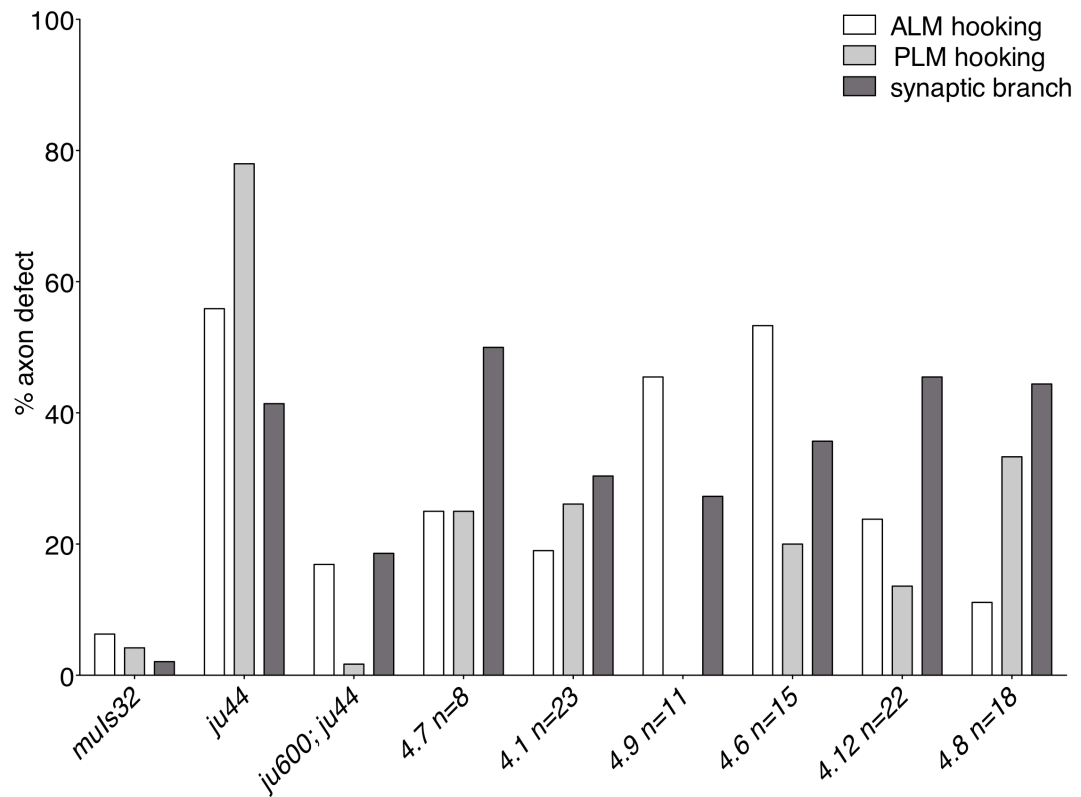
FIGURE 12. Cosmid mix 4 does not rescue *ju600.* Lines are indicated by 4.x, followed by n.
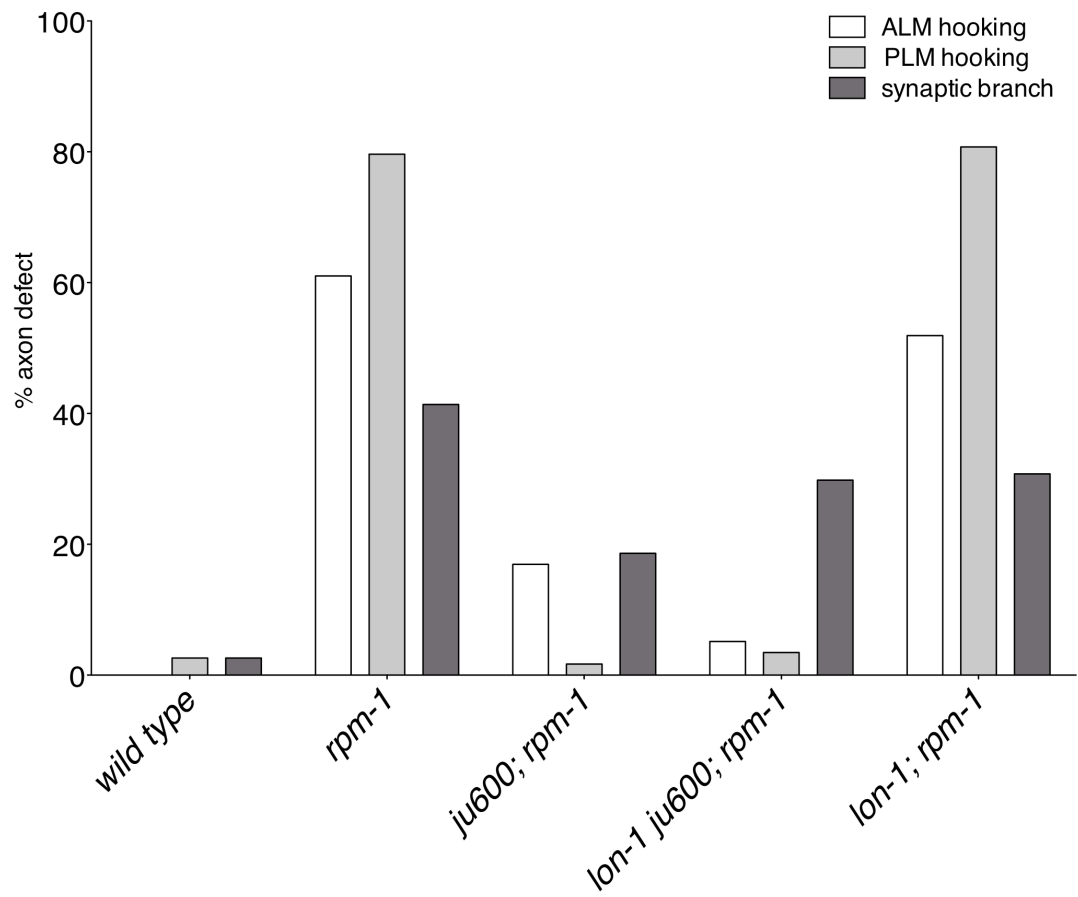
FIGURE 13. *ju600* suppresses *rpm-1* axon termination defects.

TABLE 1. Summary of *ubc* and *uev* mutant alleles

Gene (allele)	Mutation	Primer sequence & detection method	Interaction with *rpm-1*
ubc-13 (tm3380)	378 bp deletion in intron 1	YJ5577 cgattctccatttgctggtgg, YJ5578 gatttggagccgaaagaagagc, YJ5579 cgtgtaatttcttcgaaaacttctttattttcg	does not suppress
ubc-16 (ok3176)	684 bp deletion and 4bp insertion at end of exon 3 through 3'UTR	YJ5892 atgctgaatttgggtcccg YJ5893 gattccggatgataatcagaaattgataggc YJ5894 ttcggcgggagaacatagc	does not suppress
ubc-16 (ok3177)	551 bp deletion and 35 bp insertion, creates a new stop codon and results in inappropriate gene length	YJ5892 atgctgaatttgggtcccg YJ5893 gattccggatgataatcagaaattgataggc YJ5894 ttcggcgggagaacatagc	does not suppress
ubc-24 (ok3451)	~600 bp deletion from part of intron 1 to intron 4	YJ5886 caaggatgaaaggaatttggaa YJ5887 tgaatgtgcaaaaacccaaa YJ5895 gagaattggaaaccggagacc	does not suppress
ubc-25 (ok1732)	1243 bp deletion from end of exon 2 through 3' UTR	YJ4845 aatcagaagaggatggcgtg YJ4846 agagccgagacagctgagag	does not suppress
uev-1(ok2610)	496 bp deletion from promoter through part of exon 3	YJ5022 acggatttattcggatggg YJ5023 taccggggagagtaaactgg YJ5024 gtaacactttgtggcgggacc	does not suppress

Table 1, continued.

uev-3(ju587)	3' splice g→a	YJ3849 ttatatttttcgcaataaacag YJ3850 ttgtatttgaatttttaaagtg, cut with TspRI	suppresses
uev-3(ju593)	3' splice g→a	YJ3849 ttatatttttcgcaataaacag YJ3850 ttgtatttgaatttttaaagtg; sequence nt change	suppresses
uev-3(ju638)	3' splice g→a	YJ3847 aaccacaaccacgaaaaacg YJ3848 ggtggaaaagtcaggcaatg; sequence nt change	suppresses
uev-3(ju639)	26 bp deletion in exon 6	YJ7021 attcagtgggacatgcgtgg YJ7022 ccagaacgtagaaatcttgctc	suppresses

TABLE 2. DNA expression constructs

Construct name	Insert description
pCZ729 [pENTR-uev-3]	uev-3 cDNA was generated as RT-PCR product using YJ3852 ggggacaagtttgtacaaaaaagcaggctccaaaatgtccgatcaacctgg and YJ3853 ggggaccactttgtacaagaaagctgggttatgaaattccaatgacatc
pOF163 [Puev-3-GFP]	uev operon promoter (1766bp) was amplified using YJ3887 ggggacaagtttgtacaaaaaagcaggctttcgagatgtgacctggc and YJ3935 ggggaccactttgtacaagaaagctgggtccattttctaaatacaaatttg and cloned into pCZGY32 (pPD9579vGFP_GtwyB).
pCZ730 [Punc-25-GFP::UEV-3]	An entry clone containing uev-3 cDNA [pCZ729 pENTR-uev-3 cDNA] recombined with a destination vector containing 1.2kb of the unc-25 promoter and GFP labeled at the N-terminus.
pOF111 [Puev-3-uev-3]	6kb Eco 105I - Spe I fragment of cosmid F26H9 was subcloned into pSL1190, containing 1.8kb promoter of the operon, the rab-5 gene and uev-3 gene
pOF112 [Prgef-1-uev-3]	An entry clone containing uev-3 cDNA [pCZ729 pENTR-uev-3 cDNA] recombined with a destination vector containing 3.5kb of the rgef-1 promoter.
pOF113 [Prgef-1-PMK-3::GFP]	GFP was amplified and inserted into the DraIII site of vector containing 3.5kb of the rgef-1 promoter and pmk-3 cDNA, resulting in C-terminal fusion of GFP
pCZ731 [Punc-25-uev-3]	An entry clone containing uev-3 cDNA [pCZ729 pENTR-uev-3 cDNA] recombined with a destination vector containing 1.2kb of the unc-25 promoter.
pOF166 [Pmyo-3-uev-3]	An entry clone containing uev-3 cDNA [pCZ729 pENTR-uev-3 cDNA] recombined with a destination vector containing ?kb of the myo-3 promoter.
pOF176 [pBTM116-UEV-3]	An entry clone containing uev-3 cDNA [pCZ729 pENTR-uev-3 cDNA] recombined with a yeast expression destination vector containing the LexA DNA binding domain.
POF177 [pACT2-PMK-3(wt)]	An entry clone containing pmk-3 cDNA recombined with a yeast expression destination vector containing the Gal4 activation domain.

Table 2, continued.

pOF178 [pACT2-DLK-1]	An entry clone containing *dlk-1* gene [*pOF181 pENTR-dlk-1*] recombined with a yeast expression destination vector containing the Gal4 activation domain.
pOF179 [pACT2-MKK-4]	An entry clone containing *mkk-4* cDNA [*pOF180 pENTR-mkk-4*] recombined with a yeast expression destination vector containing the Gal4 activation domain.
pCZGY971 [Prgef-1-UEV-3(UEV-1 UEV)]	An entry clone containing *uev-3* cDNA was digested with *BamHI* and *SmaI* to remove UEV domain. *uev-1* UEV domain was amplified by PCR and inserted into *uev-3* entry clone. Entry clone was then recombined with destination vector containing *Prgef-1*.
pCZGY972 [Prgef-1-deltaN(uev-3)]	An entry clone containing *uev-3* cDNA was mutagenized using site directed mutagenesis to remove region N-terminal to UEV domain except for first five amino acids. Entry clone was then recombined with destination vector containing *Prgef-1*.
pCZGY974 [Prgef-1-uev-1]	*uev-1 cDNA*, as described in (Gudgen et al., 2004), was cloned into a destination vector containing *Prgef-1*.

TABLE 3. Strains and transgenic constructs

Strains	Transgene and Plasmid [DNA concentration]	Genotype
OF34	*ixEx2 [pOF163 Puev-3-GFP* 10ng/µl + pRF4 50ng/µl]	*ixEx2*
OF46	*ixEx3 [pOF111 Puev-3-uev-3* 1ng/µl + 50ng/µl pRF4]*	*uev-3(ju587); rpm-1(ju44); juIs1; ixEx3*
OF47	*ixEx4 [pOF112 Prgef-1-uev-3* 1ng/µl + 50ng/µl pRF4+ 50 ng/µl ttx-3-RFP]*	*uev-3(ju587); rpm-1(ju44); juIs1; ixEx4*
OF49	*ixEx6 [pOF166 Pmyo-3-uev-3* 1ng/µl + 50ng/µl pRF4+ 50 ng/µl ttx-3-RFP]*	*uev-3(ju587); rpm-1(ju44); juIs1; ixEx6*
OF51	*ixEx10 [pCZ731 Punc-25-uev-3* 1ng/µl + 50ng/µl pRF4+ 50 ng/µl ttx-3-RFP]*	*uev-3(ju587); rpm-1(ju44); juIs1; ixEx10*
C3442	*juEx490 [mkk-4(+)* PCR 5ng/µl + 50 ng/µl ttx-3-GFP]*	*juIs1; juEx490*
CZ3694	*juEx490[mkk-4(+)* PCR 5ng/µl + 50 ng/µl ttx-3-GFP]*	*dlk-1(ju476); juIs1; juEx490*
CZ4397	*juEx490 [mkk-4(+)* PCR 5ng/µl + 50 ng/µl ttx-3-GFP]*	*pmk-3(ju485) juIs1; juEx490*
CZ6072	*juEx490 [mkk-4(+)* PCR 5ng/µl + 50 ng/µl ttx-3-GFP]*	*uev-3(ju587); rpm-1(ju44); juIs1; juEx490*
CZ4168	*juEx669 [mkk-4(STDD)* 5ng/µl + 50 ng/µl ttx-3-RFP]*	*juIs1; juEx669*
CZ4215	*juEx669 [mkk-4(STDD)* 5ng/µl + 50 ng/µl ttx-3-RFP]*	*dlk-1(ju476); juIs1; juEx669*
CZ4398	*juEx669 [mkk-4(STDD)* 5ng/µl + 50 ng/µl ttx-3-RFP]*	*pmk-3(ju485) juIs1; juEx669*
CZ6073	*juEx669 [mkk-4(STDD)* 5ng/µl + 50 ng/µl ttx-3-RFP]*	*uev-3(ju587); rpm-1(ju44); juIs1; juEx669*
CZ8808	*juEx1685 [pCZGY971 Prgef-1-uev-3(UEV-1 UEV)* 12ng/µl + 50ng/µl ttx-3-RFP]*	*uev-3(ju639); muIs32; rpm-1(ju44); juEx1685*
CZ8911	*juEx1685 [pCZGY971 Prgef-1-uev-3(UEV-1 UEV)* 12ng/µl + 50ng/µl ttx-3-RFP]*	*muIs32; juEx1685*
CZ8812	*juEx1689 [pCZGY972 Prgef-1-uev-3(ΔN)* 10ng/µl + 50ng/µl ttx-3-RFP]*	*uev-3(ju639); muIs32; rpm-1(ju44); juEx1689*

Table 3, continued.

CZ8831	*juEx1697 [*pCZGY974 *Prgef-1-uev-1* 12ng/µl + 50 ng/µl ttx-3-RFP]	*uev-3(ju639); muIs32; rpm-1(ju44); juEx1697*
CZ12000	*juEx1697 [*pCZGY974 *Prgef-1-uev-1* 12ng/µl + 50 ng/µl ttx-3-RFP]	*muIs32; juEx1697*
CZ9478	*juEx1972 [*pCZGY *Pmec-4-uev-3* 10ng/µl + 50 ng/µl ttx-3-RFP]*	*uev-3(ju639); muIs32; rpm-1(ju44); juEx1972*
CZ11737	*juEx2582 [*pOF166 *Pmyo-3-uev-3* 1ng/µl + 50ng/µl pRF4+ 50 ng/µl ttx-3-RFP]	*uev-3(ju639); muIs32; rpm-1(ju44); juEx2582*
CZ4175	*juEx675 [*pmk-3-DraIII-GFP 50ng/µl + 50ng/µl pRF4]	*juEx675*
OF26	*juEx675 [*pmk-3-DraIII-GFP 50ng/µl + 50ng/µl pRF4]	*uev-3(ju587); juEx675*

TABLE 4. Initial arm linkage for *rpm-1* suppressors using snip-SNP mapping.

ju600	N2	CB
I-6	13	0
I+12	7	6
II-10	3	10
II+9.5	12	1
III-8	13	0
III+10	11	2
IV-7	6	7
IV+8	6	7
V-12	13	0
V+10	9	4
X-8	5	8
X+12	6	7

ju666	N2	CB
I-6	14	0
I+12	10	4
II-10	9	5
II+9.5	14	0
III-8	5	9
III+10	8	6
IV-7	8	6
IV+8	13	1
V-12	9	4
V+10	12	2
X-8	7	7
X+12	2	11

ju667	N2	CB
I-6	18	4
I+12	17	5
II-10	13	9
II+9.5	17	5
III-8	14	8
III+10	14	8
IV-7	22	21
IV+8	34	8
V-12	42	1
V+10	33	9
X-8	14	29
X+12	13	30

ju657	N2	CB
I-6	25	5
I+12	0	39
II-10	16	21
II+14	7	32
III-13	30	8
III+10	27	12
IV-7	13	26
IV+8	27	12
V-12	36	3
V+12.9	39	1
X-8	28	11
X+17	20	19

Table 4, continued.

ju660	N2	CB
I+5	6	80
I+12	6	73
I+15.5	0	86
I+26	8	77
II-10	7	7
II-5	17	33
II+1	3	10
II+14	5	9
III-13	52	30
III-1	5	9
III+10	8	6
IV-7	5	8
IV+1	10	4
IV+8	7	6
V-12.6	10	1
V-1.46	12	1
V+5	13	0
V+12.9	9	5
X-8	11	2
X+3	14	0
X+17	14	0

TABLE 5. Mapping of *ju600* recombinants on Chromosome III.

ju600	N2	CB
III-13	40	10
III-10	37	13
III-8	42	9
III-4.12	48	14
III-1.67	10	5
III-1.46	1	3
III-0.92	10	2
III-0.59	7	1
III-0.573	0	1
III-0.566	0	1
III-0.48	0	1
III-0.38	0	1
III-0.37	0	1
III-0.34	0	1
III-0.33	47	0
III-0.27	2	0
III-0.257	1	0
III-0.134	0	1
III+0.096	0	1
III+0.17	6	1
III+0.4	7	1
III+0.5	1	2
III+1.46	12	3
III+2.99	52	10
III+3.76	50	0
III+5	36	1
III+10	15	0

TABLE 6. Genes tested in MAPK/Ubiquitin RNAi screen

Clone	CGC Name	Eukaryotic Orthologous Gene Title
B0205.3	*rpn-10*	26S proteasome regulatory complex, subunit RPN10/PSMD4
B0281.3	*0*	Predicted E3 ubiquitin ligase
B0281.8	*0*	Predicted E3 ubiquitin ligase
B0391.5	*0*	Uncharacterized protein
B0391.6	*0*	Uncharacterized protein
B0393.6	*0*	0
B0403.2	*ubc-17*	Ubiquitin-conjugating enzyme
B0416.4	*0*	Predicted E3 ubiquitin ligase
B0432.13	*0*	Predicted E3 ubiquitin ligase
B0511.3	*0*	Uncharacterized protein
B0564.11	*0*	0
C01B7.6	*rpm-1*	Inhibitor of type V adenylyl cyclases/Neuronal presynaptic protein Highwire/PAM/RPM-1
C01G6.4	*0*	Predicted E3 ubiquitin ligase
C02H6.2	*0*	Uncharacterized protein
C05B10.1	*lip-1*	Dual specificity phosphatase
C05B5.5	*0*	Teneurin-1 and related extracellular matrix proteins, contain EGF-like repeats
C06A5.9	*rnf-1*	Predicted E3 ubiquitin ligase
C06E2.3	*ubc-21*	Ubiquitin-protein ligase
C06E2.7	*ubc-22*	Ubiquitin-protein ligase
C06H5.1	*0*	Uncharacterized protein
C06H5.2	*0*	Uncharacterized protein
C07G1.5	*hgrs-1*	Membrane trafficking and cell signaling protein HRS, contains VHS and FYVE domains
C08E3.10	*0*	Uncharacterized protein
C08E3.5	*0*	Uncharacterized protein
C08E3.6	*0*	Uncharacterized protein
C08E3.7	*0*	Uncharacterized protein
C08E3.8	*0*	Uncharacterized protein
C08F11.5	*0*	Uncharacterized protein
C09G12.9	*0*	Vacuolar sorting protein/ubiquitin receptor VPS23
C11H1.3	*0*	Predicted E3 ubiquitin ligase
C14B1.3	*0*	F-box domain
C15F1.5	*0*	0

Table 6, continued.

C16A3.7	*tag-182*	Transcription factor NF-X1, contains NFX-type Zn2+-binding and R3H domains
C16C10.5	*0*	Predicted RING-containing E3 ubiquitin ligase
C16C10.7	*rnf-5*	Predicted E3 ubiquitin ligase
C16C8.11	*0*	Ubiquitin and ubiquitin-like proteins
C16C8.13	*0*	Ubiquitin and ubiquitin-like proteins
C16C8.14	*0*	Ubiquitin and ubiquitin-like proteins
C16C8.4	*0*	Ubiquitin and ubiquitin-like proteins
C16C8.5	*0*	Ubiquitin and ubiquitin-like proteins
C17B7.11	*0*	Uncharacterized protein
C17C3.6	*0*	Uncharacterized protein
C17D12.5	*0*	0
C17E4.3	*0*	Protein involved in mRNA turnover and stability
C18B12.4	*0*	Predicted E3 ubiquitin ligase
C18D4.8	*srz-57*	0
C18H9.7	*rpy-1*	Acetylcholine receptor-associated protein of the synapse (rapsyn)
C25D7.4	*0*	Uncharacterized protein
C26B9.6	*0*	Predicted E3 ubiquitin ligase
C26E6.5	*fsn-1*	SOCS box protein SSB-1, contains SPRY domain
C26F1.4	*rps-30*	Ubiquitin and ubiquitin-like proteins
C28G1.1	*ubc-23*	Predicted regulator of the ubiquitin pathway (contains UAS and UBX domains)
C30F2.2	*0*	Similar to ARD GTP-binding proteins
C31C9.3	*0*	Uncharacterized protein
C31C9.4	*0*	Uncharacterized conserved protein, contains WD40 repeats and FYVE domains
C32D5.10	*0*	Predicted E3 ubiquitin ligase
C32D5.11	*0*	Predicted E3 ubiquitin ligase
C32E8.1	*0*	Predicted E3 ubiquitin ligase
C32E8.11	*0*	N-end rule pathway, recognition component UBR1
C33E10.2	*0*	Uncharacterized protein
C34B7.4	*0*	Histone acetyltransferase (MYST family)
C34D4.14	*0*	Predicted hormone receptor interactor
C34F11.1	*dsh-1*	Dishevelled 3 and related proteins
C35B1.1	*ubc-1*	Ubiquitin-protein ligase
C36A4.8	*brc-1*	Transcriptional regulator BRCA1
C36C9.3	*0*	Uncharacterized protein
C38D9.1	*0*	Uncharacterized protein

Table 6, continued.

C39B5.9	*0*	Uncharacterized protein
C39F7.2	*0*	Predicted Zn-finger protein
C44B9.4	*athp-1*	PHD Zn-finger protein
C45G7.4	*0*	Predicted E3 ubiquitin ligase
C47D12.4	*0*	Unnamed protein
C53A5.6	*0*	Proteins containing BTB/POZ and Kelch domains, involved in regulatory/signal transduction processes
C53D5.2	*0*	0
C55A6.1	*0*	Uncharacterized conserved protein
C56A3.4	*0*	Predicted E3 ubiquitin ligase
cTel54X.1	*0*	Uncharacterized protein
D1022.1	*ubc-6*	Non-canonical ubiquitin conjugating enzyme 1
D2023.5	*0*	Mercaptopyruvate sulfurtransferase/thiosulfate sulfurtransferase
D2085.4	*0*	E3 ubiquitin protein ligase
D2089.2	*0*	Protein involved in mRNA turnover and stability
F01F1.4	*rabn-5*	Rab5 GTPase effector Rabaptin-5
F01G4.2	*ard-1*	Short-chain alcohol dehydrogenase/3-hydroxyacyl-CoA dehydrogenase
F02D10.7	*0*	Transcription factor NSD1 and related SET domain proteins
F08B12.2	*prx-12*	Predicted E3 ubiquitin ligase involved in peroxisome organization
F08G12.5	*0*	0
F09C3.4	*0*	Uncharacterized protein
F09C6.2	*0*	0
F09C6.2	*0*	0
F09C6.6	*0*	Uncharacterized protein
F09D1.1	*0*	Spindle pole body protein - Sad1p
F09E5.1	*pkc-3*	Serine/threonine protein kinase
F10A3.2	*0*	Uncharacterized protein
F10A3.3	*0*	0
F11G11.9	*0*	Mercaptopyruvate sulfurtransferase/thiosulfate sulfurtransferase
F13E6.3	*0*	Chromatin remodeling protein, contains PHD Zn-finger
F14D2.11	*0*	Ubiquitin and ubiquitin-like proteins
F14D2.13	*bath-28*	0
F14H3.7	*0*	Uncharacterized protein

Table 6, continued.

F15A4.2	*0*	Unnamed protein
F15E6.1	*0*	PHD Zn-finger proteins
F16A11.1	*0*	Predicted E3 ubiquitin ligase
F16B4.8	*cdc-25.2*	M-phase inducer phosphatase
F17A2.3	*0*	Predicted helicase
F20D1.2	*0*	Uncharacterized conserved protein, contains TBC and Rhodanese domains
F21G4.4	*0*	Chromatin remodeling protein, contains PHD Zn-finger
F23C8.4	*0*	Predicted ubiquitin regulatory protein
F23D12.2	*0*	Uncharacterized protein
F25B5.4	*ubq-1*	Ubiquitin and ubiquitin-like proteins
F25D7.2	*tag-353*	Membrane-associated ER protein involved in stress response (contains ubiquitin-like domain)
F25H2.1	*tli-1*	Toll-interacting protein
F25H2.8	*ubc-25*	Predicted ubiquitin-conjugating enzyme
F26E4.11	*0*	E3 ubiquitin ligase
F26F12.7	*let-418*	Predicted helicase
F26F12.7	*let-418*	Predicted helicase
F26F4.7	*nhl-2*	Predicted E3 ubiquitin ligase
F26G5.9	*tam-1*	Predicted E3 ubiquitin ligase
F26H9.7	*uev-3*	Ubiquitin-protein ligase
F28F8.8	*0*	Uncharacterized protein
F29B9.6	*ubc-9*	Ubiquitin-protein ligase
F31D5.6	*0*	Uncharacterized protein
F31E9.1	*0*	Uncharacterized protein
F31E9.3	*0*	Uncharacterized protein
F35E12.3	*0*	Uncharacterized protein
F36A2.13	*0*	Predicted ubiquitin-protein ligase/hyperplastic discs protein, HECT superfamily
F36G9.14	*0*	Uncharacterized protein
F39B1.1	*0*	Phosphoinositide 3-kinase
F39B2.2	*uev-1*	Ubiquitin-conjugating enzyme E2
F40G9.12	*0*	Predicted E3 ubiquitin ligase
F40G9.14	*0*	Predicted E3 ubiquitin ligase
F40G9.3	*ubc-20*	Ubiquitin-protein ligase
F40G9.9	*0*	Uncharacterized protein
F42A9.2	*lin-49*	PHD finger protein BR140/LIN-49
F42C5.4	*0*	Similar to ARD GTP-binding proteins

Table 6, continued.

F42G2.5	*0*	Predicted E3 ubiquitin ligase
F42G8.6	*0*	Molybdopterin synthase sulfurylase
F43C1.5	*0*	Predicted ubiquitin-conjugating enzyme
F43C9.1	*0*	0
F43G6.6	*0*	F-box protein JEMMA and related proteins with JmjC, PHD, F-box and LRR domains
F43G6.8	*0*	Predicted E3 ubiquitin ligase
F44B9.5	*0*	Predicted phosphate acyltransferase, contains PlsC domain
F44D12.10	*0*	0
F44E7.6	*0*	Uncharacterized protein
F45C12.8	*0*	Uncharacterized protein
F45H11.2	*ned-8*	Ubiquitin-like protein
F45H7.6	*0*	Ubiquitin protein ligase RSP5/NEDD4
F46C8.5	*ceh-14*	Transcription factor LIM3, contains LIM and HOX domains
F46F2.1	*0*	Predicted E3 ubiquitin ligase
F47G9.4	*0*	Predicted E3 ubiquitin ligase
F47H4.4	*0*	Uncharacterized protein
F47H4.7	*0*	Uncharacterized protein
F47H4.8	*0*	Uncharacterized protein
F47H4.9	*0*	Uncharacterized protein
F48C1.2	*0*	Uncharacterized protein
F49C12.9	*0*	0
F49E12.4	*ubc-24*	Ubiquitin-protein ligase
F52C6.3	*0*	Ubiquitin and ubiquitin-like proteins
F52C6.4	*0*	Ubiquitin and ubiquitin-like proteins
F52D2.1	*0*	0
F52D2.10	*0*	Uncharacterized protein
F53F8.3	*0*	Predicted E3 ubiquitin ligase
F54B11.5	*0*	Predicted E3 ubiquitin ligase
F54B8.3	*0*	Uncharacterized protein
F54D10.6	*0*	Uncharacterized protein
F55A3.1	*0*	Protein involved in mRNA turnover and stability
F55G1.6	*0*	Unnamed protein
F56A3.2	*0*	GIY-YIG type nuclease
F56C3.2	*0*	Uncharacterized protein
F56D2.2	*0*	Predicted E3 ubiquitin ligase
F56D2.4	*uev-2*	Ubiquitin-protein ligase
F56F10.2	*0*	0

Table 6, continued.

F56F3.4	*0*	Predicted Zn-finger protein
F57G4.4	*0*	Uncharacterized protein
F58A4.10	*ubc-7*	Ubiquitin-protein ligase
F58G4.4	*sdz-23*	Proteins containing Ca2+-binding EGF-like domains
F59A1.7	*0*	0
F59A1.9	*0*	Uncharacterized protein
F59E10.2	*cyn-4*	Cyclophilin type, U box-containing peptidyl-prolyl cis-trans isomerase
H03G16.4	*0*	Uncharacterized protein
H05L14.2	*0*	0
H05L14.2	*0*	0
H08M01.1	*0*	Unnamed protein
H10E21.5	*0*	Predicted E3 ubiquitin ligase
H12D21.4	*0*	Mercaptopyruvate sulfurtransferase/thiosulfate sulfurtransferase
H12D21.7	*0*	Mercaptopyruvate sulfurtransferase/thiosulfate sulfurtransferase
H20J04.2	*0*	Chromatin remodeling complex WSTF-ISWI, large subunit (contains heterochromatin localization, PHD and BROMO domains)
H34C03.2	*0*	Ubiquitin C-terminal hydrolase
K03D7.7	*0*	Uncharacterized protein
K04C2.4	*brd-1*	WSN domain
K06A5.7	*cdc-25.1*	M-phase inducer phosphatase
K06A9.2	*0*	0
K09A11.5	*0*	Predicted helicase
K09F6.7	*0*	Predicted E3 ubiquitin ligase
K10B2.1	*lin-23*	Beta-TrCP (transducin repeats containing)/Slimb proteins
K12B6.8	*0*	Predicted E3 ubiquitin ligase
K12C11.2	*smo-1*	Ubiquitin-like proteins
M110.3	*0*	Uncharacterized conserved protein
M142.6	*0*	Predicted E3 ubiquitin ligase
R01H2.6	*ubc-18*	Ubiquitin-protein ligase
R02E12.4	*0*	Cystoskeletal protein Tektin
R05H5.2	*cdc-25.4*	M-phase inducer phosphatase
R06F6.2	*0*	Vacuolar assembly/sorting protein PEP5/VPS11

Table 6, continued.

R09B5.1	*0*	Uncharacterized protein
R10A10.2	*rbx-2*	SCF ubiquitin ligase, Rbx1 component
R13H4.5	*0*	Unnamed protein
R186.6	*0*	Mercaptopyruvate sulfurtransferase/thiosulfate sulfurtransferase
T01C3.3	*0*	Predicted E3 ubiquitin ligase
T01E8.4	*0*	Cdc4 and related F-box and WD-40 proteins
T01G5.7	*0*	Predicted E3 ubiquitin ligase
T02C1.1	*0*	Predicted E3 ubiquitin ligase
T05B11.1	*0*	0
T05H4.2	*0*	Uncharacterized protein
T06E6.3	*srx-40*	7-transmembrane receptor
T08D2.4	*0*	0
T08E11.7	*0*	0
T09B4.10	*chn-1*	Chaperone-dependent E3 ubiquitin protein ligase (contains TPR repeats)
T09F5.11	*0*	Uncharacterized protein
T10F2.4	*0*	mRNA splicing factor
T12B5.1	*0*	Uncharacterized protein
T12B5.10	*0*	Uncharacterized protein
T12B5.11	*0*	Uncharacterized protein
T12B5.2	*0*	Uncharacterized protein
T12B5.3	*0*	Uncharacterized protein
T12B5.4	*0*	Uncharacterized protein
T12B5.8	*0*	Uncharacterized protein
T12D8.1	*tag-350*	Putative transcription factor HALR/MLL3, involved in embryonic development
T12F5.4	*lin-59*	Putative transcription factor ASH1/LIN-59
T12G3.1	*0*	Uncharacterized conserved protein, contains ZZ-type Zn-finger
T13F3.5	*0*	0
T20F5.6	*0*	Predicted E3 ubiquitin ligase
T20F5.7	*0*	Predicted E3 ubiquitin ligase
T22B2.1	*0*	Predicted E3 ubiquitin ligase
T23B12.1	*0*	Polycomb-like PHD Zn-finger protein
T23F6.3	*0*	Unnamed protein
T24C2.4	*0*	Uncharacterized protein
T26C12.3	*0*	Ras-related GTPase
T26E3.3	*par-6*	Cell polarity protein PAR6
T27A3.2	*0*	Ubiquitin-specific protease UBP14

Table 6, continued.

T28A11.21	*0*	Uncharacterized protein
T28B11.1	*0*	0
T28C12.3	*0*	Uncharacterized protein
W02A11.3	*0*	Predicted E3 ubiquitin ligase
W04H10.3	*nhl-3*	Predicted E3 ubiquitin ligase
W05F2.5	*0*	Uncharacterized protein
W06B4.3	*0*	Vacuolar sorting protein PEP3/VPS18
W07E6.4	*prp-21*	Splicing factor 3a, subunit 1
W09G3.6	*0*	WD40 repeat-containing protein
Y102A5C.1	*0*	Uncharacterized protein
Y102A5C.10	*0*	Uncharacterized protein
Y102A5C.12	*0*	Uncharacterized protein
Y102A5C.14	*0*	Uncharacterized protein
Y102A5C.19	*0*	Uncharacterized protein
Y102A5C.3	*0*	Uncharacterized protein
Y102A5C.8	*0*	Uncharacterized protein
Y105E8A.14	*0*	0
Y110A2AR.2	*ubc-15*	Ubiquitin-protein ligase
Y113G7B.3	*0*	Uncharacterized protein
Y113G7B.4	*ftr-1*	Uncharacterized protein
Y113G7B.6	*0*	Uncharacterized protein
Y113G7B.7	*0*	Uncharacterized protein
Y116A8C.22	*0*	Chromatin remodeling protein, contains PHD Zn-finger
Y119D3A.4	*0*	0
Y119D3B.20	*0*	Uncharacterized protein
Y18D10A.18	*0*	Uncharacterized protein
Y22D7AR.9	*0*	Uncharacterized protein
Y2H9A.1	*mes-4*	Transcription factor NSD1 and related SET domain proteins
Y37E11AR.2	*0*	Zn finger protein
Y37H2C.3	*0*	Uncharacterized protein
Y38H6C.11	*0*	Uncharacterized protein
Y39A1C.2	*oxi-1*	E3 ubiquitin protein ligase
Y45F10B.8	*0*	Predicted E3 ubiquitin ligase
Y45F10C.3	*0*	Uncharacterized protein
Y46G5A.39	*0*	0
Y47G6A.14	*0*	Unnamed protein
Y47H9C.10	*0*	Uncharacterized protein
Y47H9C.11	*0*	Uncharacterized protein

Table 6, continued.

Y48G8AL.1	*0*	E3 ubiquitin protein ligase
Y49F6B.9	*0*	Predicted E3 ubiquitin ligase
Y4C6A.3	*0*	Predicted E3 ubiquitin ligase
Y51H4A.12	*0*	PHD Zn-finger proteins
Y53G8AR.5	*0*	Uncharacterized conserved protein, contains RWD domain
Y54E10BR.3	*0*	Predicted E3 ubiquitin ligase
Y54E5B.4	*ubc-16*	Ubiquitin conjugating enzyme
Y57A10A.31	*0*	Predicted E3 ubiquitin ligase
Y57A10B.1	*0*	Protein involved in mRNA turnover and stability
Y59E1A.1	*0*	Uncharacterized protein
Y63D3A.5	*tfg-1*	Unnamed protein
Y67D8C.5	*0*	E3 ubiquitin-protein ligase/Putative upstream regulatory element binding protein
Y69H2.6	*ubc-19*	Ubiquitin-conjugating enzyme-related protein Ft1, involved in programmed cell death
Y71G12B.15	*ubc-3*	0
Y71G12B.15	*ubc-3*	0
Y73C8C.7	*sdz-34*	Predicted E3 ubiquitin ligase
Y73C8C.8	*0*	Predicted E3 ubiquitin ligase
Y75B8A.10	*0*	Unnamed protein
Y75B8A.21	*0*	Uncharacterized protein
Y7A9C.1	*0*	Similar to ARD GTP-binding proteins
Y82E9BL.10	*0*	Uncharacterized protein
Y82E9BL.11	*0*	Uncharacterized protein
Y82E9BL.15	*0*	Uncharacterized protein
Y82E9BL.18	*0*	0
Y82E9BL.4	*0*	Predicted membrane protein
Y82E9BL.8	*0*	Uncharacterized protein
Y82E9BR.12	*0*	0
Y9C9A.12	*0*	Uncharacterized protein
ZC47.12	*0*	Uncharacterized protein
ZC47.3	*0*	Uncharacterized protein
ZC47.4	*0*	Uncharacterized protein
ZC47.5	*0*	Uncharacterized protein
ZC47.6	*0*	Uncharacterized protein
ZC47.7	*0*	Uncharacterized protein
ZC513.10	*0*	Uncharacterized protein
ZK1010.1	*ubq-2*	Ubiquitin/60s ribosomal protein L40 fusion
ZK1240.1	*0*	Predicted E3 ubiquitin ligase

Table 6, continued.

ZK1240.2	*0*	Predicted E3 ubiquitin ligase
ZK1240.3	*0*	Predicted E3 ubiquitin ligase
ZK1240.6	*0*	Predicted E3 ubiquitin ligase
ZK1290.9	*0*	Uncharacterized protein
ZK20.3	*0*	Nucleotide excision repair factor NEF2, RAD23 component
ZK287.5	*rbx-1*	SCF ubiquitin ligase, Rbx1 component
ZK328.6	*0*	0
ZK353.8	*0*	Ubiquitin regulatory protein UBXD2, contains UAS and UBX domains
ZK593.4	*rbr-2*	DNA-binding protein jumonji/RBP2/SMCY, contains JmjC domain
ZK637.11	*cdc-25.3*	M-phase inducer phosphatase
ZK637.14	*0*	Predicted E3 ubiquitin ligase
ZK783.4	*flt-1*	Chromatin remodeling complex WSTF-ISWI, large subunit (contains heterochromatin localization, PHD and BROMO domains)
ZK809.7	*prx-2*	Predicted E3 ubiquitin ligase
ZK945.5	*0*	Predicted E3 ubiquitin ligase
C09E7.8	*0*	Predicted E3 ubiquitin ligase
C12C8.3	*lin-41*	Predicted E3 ubiquitin ligase
C17G1.4	*0*	0
C18F10.7	*0*	Ankyrin repeat protein
C28H8.9	*0*	Predicted transcription factor Requiem/NEURO-D4
C34E10.4	*wrs-2*	Mitochondrial tryptophanyl-tRNA synthetase
F10G7.10	*0*	Predicted ubiquitin-protein ligase of the N-recognin family
F15C11.2	*0*	Ubiquitin-like protein
F25B5.4	*ubq-1*	Ubiquitin and ubiquitin-like proteins
F26H11.2	*nurf-1*	Nucleosome remodeling factor, subunit NURF301/BPTF
F29B9.2	*0*	F-box protein JEMMA and related proteins with JmjC, PHD, F-box and LRR domains
F32A6.3	*vps-41*	Vacuolar assembly/sorting protein VPS41
F36F2.3	*tag-214*	Predicted E3 ubiquitin ligase
F48E8.7	*0*	SCF ubiquitin ligase, Skp2 component

Table 6, continued.

F53H1.4	0	Chromatin remodeling complex WSTF-ISWI, large subunit (contains heterochromatin localization, PHD and BROMO domains)
F54F2.2	zfp-1	PHD finger protein AF10
F55B12.3	sel-10	Cdc4 and related F-box and WD-40 proteins
F58B6.3	par-2	Unnamed protein
F58E6.1	0	Protein involved in mRNA turnover and stability
H06I04.4	ubl-1	Ubiquitin/40S ribosomal protein S27a fusion
H39E23.1	par-1	Serine/threonine protein kinase
K02A6.3	0	Leucine rich repeat proteins, some proteins contain F-box
M02A10.3	sli-1	Tyrosine kinase negative regulator CBL
T04C10.2	epn-1	Equilibrative nucleoside transporter protein
T05A12.4	0	DEAD box-containing helicase-like transcription factor/DNA repair protein
T05H10.5	ufd-2	Ubiquitin fusion degradation protein-2
T13H2.5	0	0
T24B8.7	0	0
T28B4.1	0	Leucine rich repeat proteins, some proteins contain F-box
Y113G7B.1	0	0
Y53G8AR.2	0	PHD finger protein
Y55F3AM.6	0	Predicted E3 ubiquitin ligase
Y65B4BR.4	wwp-1	Ubiquitin protein ligase RSP5/NEDD4
ZK688.5	0	Ubiquitin-like protein, regulator of apoptosis

REFERENCES

Andersen, P.L., Zhou, H., Pastushok, L., Moraes, T., McKenna, S., Ziola, B., Ellison, M.J., Dixit, V.M., and Xiao, W. (2005). Distinct regulation of Ubc13 functions by the two ubiquitin-conjugating enzyme variants Mms2 and Uev1A. J Cell Biol *170*, 745-755.

Berman, K., McKay, J., Avery, L., and Cobb, M. (2001). Isolation and characterization of pmk-(1-3): three p38 homologs in Caenorhabditis elegans. Mol Cell Biol Res Commun *4*, 337-344.

Bloom, A.J., Miller, B.R., Sanes, J.R., and DiAntonio, A. (2007). The requirement for Phr1 in CNS axon tract formation reveals the corticostriatal boundary as a choice point for cortical axons. Genes Dev *21*, 2593-2606.

Brenner, S. (1974). The genetics of Caenorhabditis elegans. Genetics *77*, 71-94.

Broomfield, S., Chow, B.L., and Xiao, W. (1998). MMS2, encoding a ubiquitin-conjugating-enzyme-like protein, is a member of the yeast error-free postreplication repair pathway. Proc Natl Acad Sci U S A *95*, 5678-5683.

Ch'ng, Q., Williams, L., Lie, Y.S., Sym, M., Whangbo, J., and Kenyon, C. (2003). Identification of genes that regulate a left-right asymmetric neuronal migration in Caenorhabditis elegans. Genetics *164*, 1355-1367.

Chalfie, M., Tu, Y., Euskirchen, G., Ward, W.W., and Prasher, D.C. (1994). Green fluorescent protein as a marker for gene expression. Science *263*, 802-805.

Collins, C.A., Wairkar, Y.P., Johnson, S.L., and Diantonio, A. (2006). Highwire Restrains Synaptic Growth by Attenuating a MAP Kinase Signal. Neuron *51*, 57-69.

D'Souza, J., Hendricks, M., Le Guyader, S., Subburaju, S., Grunewald, B., Scholich, K., and Jesuthasan, S. (2005). Formation of the retinotectal projection requires Esrom, an ortholog of PAM (protein associated with Myc). Development *132*, 247-256.

Davis, M.W., Hammarlund, M., Harrach, T., Hullett, P., Olsen, S., and Jorgensen, E.M. (2005). Rapid single nucleotide polymorphism mapping in C. elegans. BMC Genomics *6*, 118.

Deng, L., Wang, C., Spencer, E., Yang, L., Braun, A., You, J., Slaughter, C., Pickart, C., and Chen, Z.J. (2000). Activation of the IkappaB kinase complex by TRAF6 requires a dimeric ubiquitin-conjugating enzyme complex and a unique polyubiquitin chain. Cell *103*, 351-361.

DiAntonio, A., Haghighi, A.P., Portman, S.L., Lee, J.D., Amaranto, A.M., and Goodman, C.S. (2001). Ubiquitination-dependent mechanisms regulate synaptic growth and function. Nature *412*, 449-452.

Diskin, R., Askari, N., Capone, R., Engelberg, D., and Livnah, O. (2004). Active mutants of the human p38alpha mitogen-activated protein kinase. J Biol Chem *279*, 47040-47049.

Diskin, R., Lebendiker, M., Engelberg, D., and Livnah, O. (2007). Structures of p38alpha active mutants reveal conformational changes in L16 loop that induce autophosphorylation and activation. J Mol Biol *365*, 66-76.

Garbarini, N., and Delpire, E. (2008). The RCC1 domain of protein associated with Myc (PAM) interacts with and regulates KCC2. Cell Physiol Biochem *22*, 31-44.

Garner, C.C., Waites, C.L., and Ziv, N.E. (2006). Synapse development: still looking for the forest, still lost in the trees. Cell Tissue Res *326*, 249-262.

Garrus, J.E., von Schwedler, U.K., Pornillos, O.W., Morham, S.G., Zavitz, K.H., Wang, H.E., Wettstein, D.A., Stray, K.M., Cote, M., Rich, R.L.*, et al.* (2001). Tsg101 and the vacuolar protein sorting pathway are essential for HIV-1 budding. Cell *107*, 55-65.

Giagtzoglou, N., Ly, C.V., and Bellen, H.J. (2009). Cell adhesion, the backbone of the synapse: "vertebrate" and "invertebrate" perspectives. Cold Spring Harb Perspect Biol *1*, a003079.

Grill, B., Bienvenut, W.V., Brown, H.M., Ackley, B.D., Quadroni, M., and Jin, Y. (2007). C. elegans RPM-1 Regulates Axon Termination and Synaptogenesis through the Rab GEF GLO-4 and the Rab GTPase GLO-1. Neuron *55*, 587-601.

Gudgen, M., Chandrasekaran, A., Frazier, T., and Boyd, L. (2004). Interactions within the ubiquitin pathway of Caenorhabditis elegans. Biochem Biophys Res Commun *325*, 479-486.

Guo, Q., Xie, J., Dang, C.V., Liu, E.T., and Bishop, J.M. (1998). Identification of a large Myc-binding protein that contains RCC1-like repeats. Proc Natl Acad Sci U S A *95*, 9172-9177.

Hallam, S.J., Goncharov, A., McEwen, J., Baran, R., and Jin, Y. (2002). SYD-1, a presynaptic protein with PDZ, C2 and rhoGAP-like domains, specifies axon identity in C. elegans. Nat Neurosci *5*, 1137-1146.

Hallam, S.J., and Jin, Y. (1998). lin-14 regulates the timing of synaptic remodelling in Caenorhabditis elegans. Nature *395*, 78-82.

Hart, A.C., Sims, S., and Kaplan, J.M. (1995). Synaptic code for sensory modalities revealed by C. elegans GLR-1 glutamate receptor. Nature *378*, 82-85.

Hofmann, R.M., and Pickart, C.M. (1999). Noncanonical MMS2-encoded ubiquitin-conjugating enzyme functions in assembly of novel polyubiquitin chains for DNA repair. Cell *96*, 645-653.

Horvitz, H.R., and Sulston, J.E. (1990). "Joy of the worm". Genetics *126*, 287-292.

Jin, Y. (2005). Synaptogenesis. WormBook, 1-11.

Jin, Y., and Garner, C.C. (2008). Molecular mechanisms of presynaptic differentiation. Annu Rev Cell Dev Biol *24*, 237-262.

Jones, D., Crowe, E., Stevens, T.A., and Candido, E.P. (2002). Functional and phylogenetic analysis of the ubiquitylation system in Caenorhabditis elegans: ubiquitin-conjugating enzymes, ubiquitin-activating enzymes, and ubiquitin-like proteins. Genome Biol *3*, RESEARCH0002.

Jorgensen, E.M., and Mango, S.E. (2002). The art and design of genetic screens: caenorhabditis elegans. Nat Rev Genet *3*, 356-369.

Katzmann, D.J., Odorizzi, G., and Emr, S.D. (2002). Receptor downregulation and multivesicular-body sorting. Nat Rev Mol Cell Biol *3*, 893-905.

Kennedy, S., Wang, D., and Ruvkun, G. (2004). A conserved siRNA-degrading RNase negatively regulates RNA interference in C. elegans. Nature *427*, 645-649.

Kipreos, E.T. (2005). Ubiquitin-mediated pathways in C. elegans. WormBook, 1-24.

Lewcock, J.W., Genoud, N., Lettieri, K., and Pfaff, S.L. (2007). The Ubiquitin Ligase Phr1 Regulates Axon Outgrowth through Modulation of Microtubule Dynamics. Neuron *56*, 604-620.

Li, H., Kulkarni, G., and Wadsworth, W.G. (2008). RPM-1, a Caenorhabditis elegans protein that functions in presynaptic differentiation, negatively regulates axon outgrowth by controlling SAX-3/robo and UNC-5/UNC5 activity. J Neurosci *28*, 3595-3603.

Liao, E.H., Hung, W., Abrams, B., and Zhen, M. (2004). An SCF-like ubiquitin ligase complex that controls presynaptic differentiation. Nature *430*, 345-350. Maeurer, C., Holland, S., Pierre, S., Potstada, W., and Scholich, K. (2009). Sphingosine-1-phosphate induced mTOR-activation is mediated by the E3-ubiquitin ligase PAM. Cell Signal *21*, 293-300.

Maricq, A.V., Peckol, E., Driscoll, M., and Bargmann, C.I. (1995). Mechanosensory signalling in C. elegans mediated by the GLR-1 glutamate receptor. Nature *378*, 78-81.

McCabe, B.D., Hom, S., Aberle, H., Fetter, R.D., Marques, G., Haerry, T.E., Wan, H., O'Connor, M.B., Goodman, C.S., and Haghighi, A.P. (2004). Highwire regulates presynaptic BMP signaling essential for synaptic growth. Neuron *41*, 891-905.

Moraes, T.F., Edwards, R.A., McKenna, S., Pastushok, L., Xiao, W., Glover, J.N., and Ellison, M.J. (2001). Crystal structure of the human ubiquitin conjugating enzyme complex, hMms2-hUbc13. Nature structural biology *8*, 669-673.

Murthy, V., Han, S., Beauchamp, R.L., Smith, N., Haddad, L.A., Ito, N., and Ramesh, V. (2004). Pam and its ortholog highwire interact with and may negatively regulate the TSC1.TSC2 complex. J Biol Chem *279*, 1351-1358.

Nakata, K., Abrams, B., Grill, B., Goncharov, A., Huang, X., Chisholm, A.D., and Jin, Y. (2005). Regulation of a DLK-1 and p38 MAP kinase pathway by the ubiquitin ligase RPM-1 is required for presynaptic development. Cell *120*, 407-420.

Nonet, M.L. (1999). Visualization of synaptic specializations in live C. elegans with synaptic vesicle protein-GFP fusions. J Neurosci Methods *89*, 33-40.

Pickart, C.M. (2001). Mechanisms underlying ubiquitination. Annu Rev Biochem *70*, 503-533.

Pickart, C.M., and Eddins, M.J. (2004). Ubiquitin: structures, functions, mechanisms. Biochim Biophys Acta *1695*, 55-72.

Pierre, S., Maeurer, C., Coste, O., Becker, W., Schmidtko, A., Holland, S., Wittpoth, C., Geisslinger, G., and Scholich, K. (2008). Toponomics analysis of functional interactions of the ubiquitin ligase PAM (Protein Associated with Myc) during spinal nociceptive processing. Mol Cell Proteomics *7*, 2475-2485.

Po, M.D., Hwang, C., and Zhen, M. (2010). PHRs: bridging axon guidance, outgrowth and synapse development. Curr Opin Neurobiol *20*, 100-107.

Raman, M., Chen, W., and Cobb, M.H. (2007). Differential regulation and properties of MAPKs. Oncogene *26*, 3100-3112.

Remy, I., and Michnick, S.W. (2004). Regulation of apoptosis by the Ft1 protein, a new modulator of protein kinase B/Akt. Mol Cell Biol *24*, 1493-1504.

Saiga, T., Fukuda, T., Matsumoto, M., Tada, H., Okano, H.J., Okano, H., and Nakayama, K.I. (2009). Fbxo45 forms a novel ubiquitin ligase complex and is required for neuronal development. Mol Cell Biol *29*, 3529-3543.

Sancho, E., Vila, M.R., Sanchez-Pulido, L., Lozano, J.J., Paciucci, R., Nadal, M., Fox, M., Harvey, C., Bercovich, B., Loukili, N.*, et al.* (1998). Role of UEV-1, an inactive variant of the E2 ubiquitin-conjugating enzymes, in in vitro differentiation and cell cycle behavior of HT-29-M6 intestinal mucosecretory cells. Mol Cell Biol *18*, 576-589.

Sanford, T., Golomb, M., and Riddle, D.L. (1983). RNA polymerase II from wild type and alpha-amanitin-resistant strains of Caenorhabditis elegans. J Biol Chem *258*, 12804-12809.

Sarin, S., Prabhu, S., O'Meara, M.M., Pe'er, I., and Hobert, O. (2008). Caenorhabditis elegans mutant allele identification by whole-genome sequencing. Nat Methods *5*, 865-867.

Schaefer, A.M., Hadwiger, G.D., and Nonet, M.L. (2000). rpm-1, a conserved neuronal gene that regulates targeting and synaptogenesis in C. elegans. Neuron *26*, 345-356.

Scholich, K., Pierre, S., and Patel, T.B. (2001). Protein associated with Myc (PAM) is a potent inhibitor of adenylyl cyclases. J Biol Chem *276*, 47583-47589.

Serra-Pages, C., Medley, Q.G., Tang, M., Hart, A., and Streuli, M. (1998). Liprins, a family of LAR transmembrane protein-tyrosine phosphatase-interacting proteins. J Biol Chem *273*, 15611-15620.

Simmer, F., Tijsterman, M., Parrish, S., Koushika, S.P., Nonet, M.L., Fire, A., Ahringer, J., and Plasterk, R.H. (2002). Loss of the putative RNA-directed RNA polymerase RRF-3 makes C. elegans hypersensitive to RNAi. Curr Biol *12*, 1317-1319.

Skaug, B., Jiang, X., and Chen, Z.J. (2009). The role of ubiquitin in NF-kappaB regulatory pathways. Annu Rev Biochem *78*, 769-796.

Tavernarakis, N., Wang, S.L., Dorovkov, M., Ryazanov, A., and Driscoll, M. (2000). Heritable and inducible genetic interference by double-stranded RNA encoded by transgenes. Nat Genet *24*, 180-183.

Timmons, L., and Fire, A. (1998). Specific interference by ingested dsRNA. Nature *395*, 854.

VanDemark, A.P., Hofmann, R.M., Tsui, C., Pickart, C.M., and Wolberger, C. (2001). Molecular insights into polyubiquitin chain assembly: crystal structure of the Mms2/Ubc13 heterodimer. Cell *105*, 711-720.

Wan, H.I., DiAntonio, A., Fetter, R.D., Bergstrom, K., Strauss, R., and Goodman, C.S. (2000). Highwire regulates synaptic growth in Drosophila. Neuron *26*, 313-329.

Wang, C., Deng, L., Hong, M., Akkaraju, G.R., Inoue, J., and Chen, Z.J. (2001). TAK1 is a ubiquitin-dependent kinase of MKK and IKK. Nature *412*, 346-351.

Wang, J., and Barr, M.M. (2005). RNA interference in Caenorhabditis elegans. Methods Enzymol *392*, 36-55.

White, J.G., E. Southgate, J. N. Thomson, and S. Brenner (1976). The Structure of the Ventral Nerve Cord of Caenorhabditis elegans. Pilos Trans R Soc Lond B Biol Sci *275*, 327-348.

Whitmarsh, A.J. (2006). The JIP family of MAPK scaffold proteins. Biochem Soc Trans *34*, 828-832.

Wicks, S.R., Yeh, R.T., Gish, W.R., Waterston, R.H., and Plasterk, R.H. (2001). Rapid gene mapping in Caenorhabditis elegans using a high density polymorphism map. Nat Genet *28*, 160-164.

Wu, C., Daniels, R.W., and DiAntonio, A. (2007). DFsn collaborates with Highwire to down-regulate the Wallenda/DLK kinase and restrain synaptic terminal growth. Neural Dev *2*, 16.

Xiao, W., Lin, S.L., Broomfield, S., Chow, B.L., and Wei, Y.F. (1998). The products of the yeast MMS2 and two human homologs (hMMS2 and CROC-1) define a structurally and functionally conserved Ubc-like protein family. Nucleic acids research *26*, 3908-3914.

Yan, D., Wu, Z., Chisholm, A.D., and Jin, Y. (2009). The DLK-1 kinase promotes mRNA stability and local translation in C. elegans synapses and axon regeneration. Cell *138*, 1005-1018.

Zhai, R.G., and Bellen, H.J. (2004). The architecture of the active zone in the presynaptic nerve terminal. Physiology (Bethesda) *19*, 262-270.

Zhen, M., Huang, X., Bamber, B., and Jin, Y. (2000). Regulation of presynaptic terminal organization by C. elegans RPM-1, a putative guanine nucleotide exchanger with a RING-H2 finger domain. Neuron *26,* 331-343.

Zhen, M., and Jin, Y. (1999). The liprin protein SYD-2 regulates the differentiation of presynaptic termini in C. elegans. Nature *401*, 371-375.